Molecular Biology of the Cell
Vol. 20, 3583–3597, August 1, 2009

# A Phosphatidylinositol-Transfer Protein and Phosphatidylinositol-4-phosphate 5-Kinase Control Cdc42 to Regulate the Actin Cytoskeleton and Secretory Pathway in Yeast

**Liat Yakir-Tamang and Jeffrey E. Gerst**

Department of Molecular Genetics, Weizmann Institute of Science, Rehovot 76100, Israel

Submitted October 28, 2008; Revised May 7, 2009; Accepted May 20, 2009
Monitoring Editor: Thomas F.J. Martin

**The actin cytoskeleton rapidly depolarizes in yeast secretory (*sec*) mutants at restrictive temperatures. Thus, an unknown signal conferred upon secretion is necessary for actin polarity and exocytosis. Here, we show that a phosphatidylinositol (PI) transfer protein, Sfh5, and a phosphatidylinositol-4-phosphate 5-kinase, Mss4, facilitate Cdc42 activation to concomitantly regulate both actin and protein trafficking. Defects in Mss4 function led to actin depolarization, an inhibition of secretion, reduced levels of phosphatidylinositol 4,5-bisphosphate [PI(4,5)$P_2$] in membranes, mislocalization of a pleckstrin homology domain fused to green fluorescent protein, and the mislocalization of Cdc42. Similar defects were observed in *sec*, *myo2-66*, and *cdc42-6* mutants at elevated temperatures and were rescued by the overexpression of *MSS4*. Likewise, the overexpression of *SFH5* or *CDC42* could ameliorate these defects in many *sec* mutants, most notably in *sec3*Δ cells, indicating that Cdc42-mediated effects upon actin and secretion do not necessitate Sec3 function. Moreover, mutation of the residues involved in PI binding in Sfh5 led to the mislocalization and loss of function of both Sfh5 and Cdc42. Based upon these findings, we propose that the exocytic signal involves PI delivery to the PI kinases (i.e., Mss4) by Sfh5, generation of PI(4,5)$P_2$, and PI(4,5)$P_2$-dependent regulation of Cdc42 and the actin cytoskeleton.**

## INTRODUCTION

Polarized growth is necessary for a variety of processes in eukaryotic cells (e.g., cell division, morphogenesis, and motility) and involves conserved signaling pathways that regulate the cytoskeleton and secretory pathway. In *Saccharomyces cerevisiae*, asymmetric distribution of the actin cytoskeleton is essential for the establishment and maintenance of cell polarity and for targeting secretory vesicles to the bud (Irazoqui and Lew, 2004; Pruyne *et al*., 2004). Yeast actin cytoskeleton mutants accumulate secretory vesicles, are secretion defective, and exhibit other phenotypes consistent with defects in polarized growth (Irazoqui and Lew, 2004; Pruyne *et al*., 2004).

All yeast secretory (*sec*) mutants examined affect actin polarity at elevated temperatures, and some even at temperatures permissive for growth (Aronov and Gerst, 2004). The rapidity in which defects in actin are observed in temperature-shifted *sec* mutants led us to hypothesize that there is an explicit signal sent to the actin regulatory machinery to maintain polarity and exocytosis (Aronov and Gerst, 2004). This "exocytic signal" is predicted to be generated upon vesicle docking or fusion and is blocked immediately upon a cessation in vesicle transport. Given the connection between polyphosphoinositide generation and the control of actin (Yin and Janmey, 2003; Downes *et al*., 2005), we postulated that this pathway might transduce the occurrence of fusion events at the site of exocytosis to the actin cytoskeleton, via their known regulators and effectors (Aronov and Gerst, 2004). Thus, the exocytic signal could represent a phosphoinositide (PI)-mediated signal sent to the actin cytoskeleton as well as other cellular processes to maintain polarized growth and secretion.

PIs are regulators of diverse cellular processes in eukaryotic cells. In particular, phosphatidylinositol 4,5-bisphosphate [PI(4,5)$P_2$], a major polyphosphoinositide, regulates actin organization, regulated exocytosis, endocytosis, and cell growth (Yin and Janmey, 2003; Downes *et al*., 2005). Because PI(4,5)$P_2$ is synthesized at specific sites within the cell, transient changes in its local concentration lead to the recruitment and activation of signaling proteins and induction of site-specific responses. PI(4,5)$P_2$ controls both membrane recruitment and the activation of proteins bearing specific domains for lipid recognition (i.e., pleckstrin homology [PH] domains) (Lemmon and Ferguson, 2000). For example, PI(4,5)$P_2$ binds to actin regulatory proteins, such as profilin and gelsolin, and modulates their ability to polymerize actin (Yin and Janmey, 2003). PI(4,5)$P_2$-binding proteins are directly involved in regulated exocytosis in higher eukaryotes. For example, $Ca^{2+}$-dependent activator protein for secretion (CAPS) is a PH domain-containing activator of $Ca^{2+}$-dependent exocytosis that requires PI(4,5)$P_2$ to elicit dense core vesicle release (Grishanin *et al*., 2004). Moreover, PI(4,5)$P_2$ levels are inhibitory to soluble *N*-ethylmaleimide-sensitive factor attachment protein receptor (SNARE)-mediated fusion in the absence of CAPS (James *et al*., 2008). In contrast to mammalian cells, no secretion factors have been shown to require PI(4,5)$P_2$ binding to confer constitutive exocytosis in yeast. However, numerous plasma membrane (PM)-associated proteins that affect actin contain PH do-

This article was published online ahead of print in *MBC in Press* (http://www.molbiolcell.org/cgi/doi/10.1091/mbc.E08–10–1073) on May 28, 2009.

Address correspondence to: Jeffrey E. Gerst (jeffrey.gerst@weizmann.ac.il).

**Table 1.** Yeast strains used in this study

| Strain | Genotype | Source |
|---|---|---|
| W303a | *MAT*a *ade2 can1 his3 leu2 lys2 trp1 ura3* | J. Hirsch (Mount Sinai School of Medicine) |
| AAY202 | *MAT*α *leu2-3, 112 ura3-52 his3-*Δ*200 trp1-*Δ*901 lys2-801 suc2-*Δ*9 mss4::HIS3MX6* YCplac mss4-102 (*LEU2, CEN6, mss4-102)* | S. Emr (Cornell University) |
| *cdc42-6* | *MAT*a *his2 trp1-289 ura3-52 URA3::cdc42-6, GAL1p-CDC42::LEU2* | P. Brennwald, (University of North Carolina, Chapel Hill) |
| *cdc24-1* | *MAT*a *leu2 cdc24-1* | M. Wigler (Cold Spring Harbor Laboratory) |
| NY1002 | *MAT*a *his3 leu2 trp1 ura3-52 myo2-66* | P. Novick (University of California, San Diego) |
| DBY1885 | *MAT*a *ura3-52 sac1-6* | P. Novick |
| H2 | *MAT*a *his4-580 leu2-3,112 trp1-289 ura3-52 sec1-1* | S. Keranen (VTT Biotechnology) |
| NY770 | *MAT*a *leu2-3,112 ura3-52 sec2-41* | P. Novick |
| NY412 | *MAT*a *leu2-3,112 ura3-52 sec3-2* | P. Novick |
| NY2450 | *MAT*a *his3*Δ*200 leu2-3,112 ura3-5 sec3*Δ*::kanMX4* | P. Novick |
| NY774 | *MAT*a *ura3-52 leu2-3,112 sec4-8* | P. Novick |
| NY778 | *MAT*α *leu2-3, 112 ura3-52 sec6-4* | P. Novick |
| ABY717 | *MAT*a *leu2 ura3 trp1-1 sec6-4 end4-1* | E. Harsay (University of Kansas) |
| NY780 | *MAT*a *leu2-3,112 ura3-52 sec8-9* | P. Novick |
| NY782 | *MAT*a *leu2-3,112 ura3-52 sec9-4* | P. Novick |
| RSY941 | *MAT*a *leu2-3,112 ura3-52 sec12-1* | R. Schekman (University of California at Berkeley) |
| VLSec22 | *MAT*a *leu2-3,112 ura3-52 trp1 his3 sec22-2* | J. Gerst (Weizmann Institute of Science) |

mains (i.e., Slm1, Slm2, Boi1, Boi2, Cla4, Bem3, and Rom2) and may play a supportive role in exocytosis. Thus, PI(4,5)$P_2$ synthesis and binding could be necessary for vesicle trafficking and secretion in yeast.

In higher eukaryotes, PI(4,5)$P_2$ is synthesized from phosphatidylinositol-4-phosphate [PI(4)P], by using phosphatidylinositol-4-phosphate 5-kinase [PI(4)P 5-kinase], or from phosphatidylinositol-5-phosphate, using phosphatidylinositol-5-phosphate 4-kinase (Doughman *et al*., 2003). In *S. cerevisiae*, a PI(4)P 5-kinase, Mss4, synthesizes the PI(4,5)$P_2$ pool at the PM, and a temperature-sensitive (ts) mutation in its gene results in actin delocalization, sporulation defects, and cell death at restrictive temperatures (Desrivieres *et al*., 1998). Mss4 localizes primarily to the PM, although phosphorylation-dependent shuttling between the PM and nucleus was reported previously (Audhya and Emr, 2003). PI(4,5)$P_2$ synthesis in yeast stimulates the Rho1/2 GTPases, resulting in activation of Pkc1 and the downstream mitogen-activated protein kinase cascade involved in cell wall integrity (Levin, 2005; Strahl and Thorner, 2007). The signaling pathway mediated by Rho1 is needed for proper actin organization (Levin, 2005), and Mss4 may control actin by mediating recruitment of the guanosine triphosphate exchange factor (GEF) of Rho1, Rom2, to the PM via PI(4,5)$P_2$ binding to its PH domain (Audhya and Emr, 2002). Rom2, in turn, activates Rho1/2 at the PM to regulate actin organization, cell wall integrity, and cell polarity (Levin, 2005; Strahl and Thorner, 2007). Another Rho family GTPase, Cdc42, and its PH domain-containing GEF, Cdc24, are necessary for polarization of actin in yeast. Cdc42 and Cdc24 are essential factors for assembly of the polarized patch (Etienne-Manneville, 2004), and activated Cdc42 recruits the Wiskott–Aldrich syndrome protein (WASP) orthologue Bee1, WASP-interacting protein Vrp1, and type I myosins to the site of polarization to facilitate actin polymerization (Lechler *et al*., 2001; Etienne-Manneville, 2004). In addition, Cdc42 was shown recently to act in concert with PI(4,5)$P_2$ to regulate the polarized localization of the Cdc42 effector Gic2 during polarized cell growth in yeast (Orlando *et al*., 2008).

We now demonstrate a role for PI(4,5)$P_2$ synthesis and signaling in the regulation of exocytosis in yeast. *MSS4* overexpression rescues mutants of the secretory pathway at semirestrictive temperatures and restores actin polarity. A mutation in *MSS4* is synthetic lethal with secretory mutants, mislocalizes actin, PH domain-containing proteins and Cdc42, and is defective in secretion at elevated temperatures. These defects are directly related to PI(4,5)$P_2$ synthesis by Mss4 and can be compensated for in certain *sec* mutants by overexpression of a nonclassical PI transfer protein (PITP) Sfh5 (Routt *et al*., 2005). Sfh5 stimulates Stt4, the PI 4-kinase that acts upstream to Mss4 (Routt *et al*., 2005), and we show here that it localizes to the PM in a manner dependent upon the actin cytoskeleton and secretory pathway. Mutations in the putative PI-binding domain of Sfh5 abolish both its delivery to the PM and ability to rescue *sec* and *cdc42-6* mutants at elevated temperatures. We propose that vesicle fusion at the PM allows Sfh5 to deliver PI to Stt4/Mss4 generate PI(4,5)$P_2$ and thus regulate actin polarization (via Cdc42 and other Rho family members) and to maintain exocytosis. Thus, the secretory pathway regulates the actin cytoskeleton and vice versa. Moreover, because the overexpression of *SFH5*, *MSS4*, or *CDC42* ameliorates the growth defects of *sec3*Δ cells, it indicates that Cdc42-mediated restoration of actin and secretion does not necessitate Sec3 function. Because Sec3 has been proposed to bind both Cdc42 and PI(4,5)$P_2$ (Zhang *et al*., 2008), our results imply that Cdc42 mediates growth functions independently of Sec3.

## MATERIALS AND METHODS

### *Media, DNA, and Genetic Manipulations*

Yeast were grown in standard growth media containing 2% glucose. Synthetic complete and drop-out media were prepared similar to that described previously (Rose *et al*., 1990). Standard methods were used for the introduction of DNA into yeast and the preparation of genomic DNA (Rose *et al*., 1990). Cells transformed with genes under the control of the *MET25* promoter were switched to synthetic medium lacking methionine for 1–2 h to induce the expression of green fluorescent protein (GFP)-tagged proteins. Cells transformed with genes under the control of a galactose-inducible promoter were grown in galactose (3.5%)-containing media for 8 h. Standard procedures were used for performing genetic crosses and the isolation of meiotic segregants. Growth phenotypes of the segregants were assessed by replica plating colonies that germinated at 26°C onto YPD plates at 26 and 37°C. A minimum of 10 informative tetrads were dissected for each cross.

### *Yeast Strains*

Yeast strains used are listed in Table 1.

**Table 2.** Plasmids used in this study

| Name | Gene-expressed | Vector | Insertion sites | Source |
|---|---|---|---|---|
| pRS426GFP-2PH (PLCδ)[a] | *GFP-2XPH* (PLCδ) | pRS426 (2μ ,*URA3*) | BglII and SalI | S. Emr (Cornell University) |
| pRS426MSS4 | *MSS4* | pRS426 | BamHI and SacI | This study |
| pUG35MSS4 | *MSS4-GFP* | pUG35[b] (*MET25*::*CEN, yEGFP, URA3*) | BamHI and SalI | This study |
| pUG35CDC24 | *CDC24-GFP* | pUG35 | BamHI and SalI | This study |
| pUG36CDC42 | *GFP-CDC42* | pUG36[b] (*MET25*::*yEGFP, CEN, URA3*) | BamHI and EcoRI | This study |
| pUG36ROM2 | *GFP-ROM2* | pUG36 | BamHI and XhoI | This study |
| pUG36SFH5 | *GFP-SFH5* | pUG36 | BamHI and XhoI | This study |
| pUG36SFH5$^{K236A}$ | *GFP-SFH5$^{K236A}$* | pUG36 | BamHI and XhoI | This study |
| pUG36SFH5$^{E204A,K236A}$ | *GFP- SFH5$^{E204A,K236A}$* | pUG36 | BamHI and XhoI | This study |
| pAD54SFH5 | *GFP-SFH5* | pAD54 | SalI and SacI | This study |
| PAD54SFH5$^{E204A,K236A}$ | *GFP- SFH5$^{E204A,K236A}$* | pAD54 | SalI and SacI | This study |
| pAD54MSS4 | *MSS4* | pAD54 | SalI and SacI | This study |
| pAD54-RFP-CDC42 | *CDC42* | pAD54 | SalI and SacI | J. Gerst (Weizmann Institute of Science) |
| pAD54-RFP-YIF1 | *RFP-YIF1* | pAD54 | SalI and SacI | J. Gerst |
| pAD54-RFP-SNX4 | *RFP-SNX4* | pAD54 | SalI and SacI | J. Gerst |
| pGBK-MSS4 | *MSS4* | pGBK T7 | BamHI and SalI | This study |
| pSM1960-SEC63-RFP | *SEC63-RFP* | pSM1960 | | S. Michaelis (Johns Hopkins University) |
| pUG36SUC2 | *GFP-SUC2* | pUG36 | XhoI and SalI | This study |
| BG1805SFH5 | *GST-SFH5* | BG1805 | | MORF collection (Gelperin et al., 2005) |

[a] Plasmid described in Stefan et al. (2002).
[b] Plasmids described in Longtine et al. (1998).

### *Plasmids*

Plasmids and vectors used in this study are listed in Table 2. Point mutations in *SFH5* were generated in plasmid pUG36SFH5 by *Pfu*-mediated site-directed mutagenesis. Plasmid pUG36SFH5$^{K236A}$ was generated from pUG36SFH5 by using forward and reverse primers for K236A (5′-CCACCAG-AAAGGCGTTCGTTCGTGGTATTAAC-3′ and 5′-GTTAATAC-CACGAACGCC-TTTCTGGTGG-3′), and pUG36SFH5$^{E204A,K236A}$ was generated from pUG36SFH5$^{K236A}$ using forward and reverse primers for E204A (5′-CTTTCAAAAATACTATCCAGCACTGTTATATGCAAAG-3′ and 5′-CTTTGCA-TATAACAGTGCTGGATAGTATTTTTGAAAG-3′).

### *Actin Staining*

The actin cytoskeleton was stained with rhodamine-conjugated phalloidin (Sigma-Aldrich, St. Louis, MO). Cells were grown to $OD_{600}$ = 0.5 in YPD and fixed with formaldehyde at a final concentration of 4% for 1 h. Cells were harvested, washed twice with 1× phosphate-buffered saline (PBS), permeablized using 0.5% NP-40 in PBS for 5min, and washed again with 1× PBS. For staining, 100-μl aliquots were incubated with rhodamine-conjugated phalloidin (final concentration of 0.165 μM) for 15–60 min on ice and washed with 1× PBS. Cells were mixed 1:1 with mounting medium and mounted on slides before visualization. To obtain quantitative data on the organization of actin, 50–100 cells of each strain were scored for the distribution of actin patches to the mother or bud.

### *Microscopy*

Fluorescence imaging was performed using an LSM confocal microscope with LSM510 software (Carl Zeiss, Jena, Germany). The following wavelengths were used: rhodamine-phalloidin (excitation, 545 nm; emission, 560–580 nm) and GFP (excitation, 480 nm; emission, 530 nm). For live-cell imaging, cells were grown to mid-log phase on selective synthetic medium containing methionine and transferred to medium lacking methionine for 1–2 h before visualization to induce expression from the *MET25* promoter. For temperature-sensitive strains, cells were either maintained at 26°C or shifted to 37°C for an additional 45 min. Shown in the figures are representative images of individual cells along with their corresponding statistics for protein localization (Figures 3, A B, and D; 5A; 6, B and D; 7, C and D; and Supplemental Figures S1 and S2, A and C) or integrity of the actin cytoskeleton (Figure 2), as determined from 100 cells counted for each strain.

### *Cell Fractionation and PI(4,5)$P_2$ Detection in Dot Blots*

Subcellular fractionation of yeast cells was performed by standard techniques. In brief, 25 $OD_{600}$ units of cells was harvested in mid-log phase and lysed using glass beads in 300 μl of lysis buffer containing 25 mM potassium phosphate, pH 7.0, 100 mM NaCl, 2 mM EDTA, and the following protease inhibitors: aprotinin (1 μg/ml), leupeptin (2 μg/ml), pepstatin (1 μg/ml), soybean trypsin inhibitor (10 μg/ml), and phenylmethylsulfonyl fluoride (1 mM). After lysis, equivalent (protein) amounts of cell extracts were centrifuged at 1500 × *g* for 4 min to remove intact cells and cell wall debris to yield the total cell lysate (TCL); the latter was then centrifuged at 10,000 × *g* for 10 min to yield the S10 supernatant and P10 pellet fractions. The S10 was centrifuged at 100,000 × *g* for 1 h to yield the S100 supernatant and P100 pellet fractions. The pellet fractions were solubilized with 50 μl of lysis buffer containing SDS (1% final concentration). Protein determination was performed using the microbicinchoninic acid technique (Pierce Chemical, Rockford, IL). The TCLs and different subcellular fractions were diluted with lysis buffer, and 1-μl aliquots containing 0.5 μg of protein were carefully spotted onto nitrocellulose membranes (Whatman Schleicher and Schuell, Dassel, Germany). In parallel, we used an array of eight phosphoinositide standards preblotted onto a nitrocellulose membrane in increasing concentrations (PIP Array; Echelon Biosciences, Salt Lake City, UT). Both nitrocellulose membranes were first blocked in Tris-buffered saline solution (TBST: 20 mM Tris-HCl, pH 7.4, 150 mM NaCl, and 0.5% Tween 20) containing 0.5% nonfat milk for 1 h and then incubated overnight with a mouse monoclonal anti-$PIP_2$ antibody (catalog no. 915-052; Assay Designs, Ann Arbor, MI) diluted 1:5000 in TSBT. Next, blots were washed (4 times) with TBST and incubated with a horseradish peroxidase-conjugated sheep anti-mouse secondary antibody (1: 10,000; GE Healthcare, Little Chalfont, Buckinghamshire, United Kingdom) for 1 h, washed in TBST (4 times), and detected by chemiluminescence (enhanced chemiluminescence Western blotting detection reagents; GE Healthcare). Optical density measurements of the exposed films were made using Image Gauge V3.01 software (Fujifilm, Tokyo, Japan), and the values were normalized for background.

### *Cell Fractionation and Protein Detection in Blots*

Subcellular fractionation of yeast by using differential centrifugation was performed as detailed above. Samples of equal amounts of protein (30 μg) obtained from the different fractions were resolved by SDS-polyacrylamide gel electrophoresis (PAGE), and detected in blots (as described above) by using anti-glutathione transferase (GST) (1:1000), and anti-GFP (1:1000), anti-Dpm1 (1:1000), anti-Sso1 (1:3000), anti-Sed5 (1:3000), and anti-Ufe1 (1:1000) antibodies by chemiluminescence. Protein expression levels were determined by densitometric analysis of bands in Western blots using TINA 2.0 software (Raytest, Straubenhardt, Germany). Band density was normalized for changes in protein expression in the TCLs. Measurements are expressed in arbitrary units.

### *Antibodies*

Protein detection in blots was performed using monoclonal antibodies anti-GST (1:1000; Santa Cruz Biotechnology, Santa Cruz, CA) and anti-GFP (1:1000; Roche Diagnostics, Indianapolis, IL) and polyclonal antibodies anti-Sed5 (1:3000; a gift from H. Pelham, Medical Research Council Laboratory for Molecular Biology, Cambridge, United Kingdom), anti-Dpm1 (1:1000; Invitrogen, Carlsbad, CA), anti-Sso (1:3000) (a gift from S. Keranen, VTT Biotechnology, Espoo, Finland), anti-Ufe1 (1:1000; a gift from H. Pelham), peroxidase-conjugated sheep anti-mouse secondary antibody (1:10,000; GE Healthcare), and anti-PI(4,5)$P_2$ (1:5000; Assay Designs).

### *Invertase Assay*

Invertase secretion was measured as described previously (Goldstein and Lampen, 1975). Secreted and nonsecreted activities were determined from glucose-repressed and derepressed cells and measured in units based upon absorption at 540 nm (1 U = 1 mol glucose released/min/100 mg dry cells).

## RESULTS

### *MSS4 Overexpression Restores the Growth of Secretory Mutants*

Mss4 regulates actin organization by generating PI(4,5)$P_2$ (Desrivieres *et al*., 1998). To determine whether the putative exocytic signal is mediated by PI(4,5)$P_2$, we tested for genetic interactions between *MSS4* and genes of the secretory pathway. To characterize the effects of *MSS4* overexpression on the growth of *sec* mutants, we transformed yeast containing mutations in SNAREs (e.g., *sec22-2* and *sec9-4* cells), SNARE regulatory proteins (e.g., *sec1-1* cells), a secretory GTPase (e.g., *sec4-8* cells), Exocyst components (e.g., *sec3-2*, *sec8-9*, and *sec15-2* cells), a GEF essential for vesicle budding from the ER (e.g., *sec12-1* cells), a type V myosin involved in secretory vesicle transport (e.g., *myo2-66* cells), and a Rho family GTPase involved in actin regulation and vesicle transport (e.g., *cdc42-6* cells) with either a multi-copy vector expressing *MSS4* or vector alone and performed growth tests (Figure 1). Although this work was in progress, Bankaitis and colleagues found that *MSS4* overexpression rescued the growth defects of several late secretory mutants at the semirestrictive and restrictive temperatures (i.e., *sec2-41*, *sec8-9*, *sec9-4*, and *sec15-1* cells) (Routt *et al*., 2005). We found that *MSS4* overexpression greatly ameliorated the growth of both late (e.g., *sec3-2*, *sec4-8*, *sec8-9*, *sec15-2*, and *myo2-66* cells) and early *sec* mutants (e.g., *sec12-1* and *sec22-2* cells) at restrictive temperatures (Figure 1A). In addition, a milder rescue was observed at semirestrictive temperatures in *sec1-1*, *sec3*Δ and *sec9-4* cells overexpressing *MSS4* (Figure 1A; data not shown; Coluccio *et al*., 2004; Routt *et al*., 2005). Interestingly, a mutant in *cdc42-6* that has been proposed by others to affect exocytosis, but not actin, was also strongly rescued by *MSS4* overexpression (Figure 1A). *MSS4* overexpression also fully restored the growth of *mss4-102* cells at restrictive temperatures (37°C) but had no effect upon the growth of wild-type (WT) cells (Figure 1A). Thus, Mss4 overproduction alleviates secretion-related growth defects in both *sec* and *cdc42-6* mutants. This is unlikely to be connected to the control of endocytosis because *MSS4* overexpression did not have differential effects upon *sec6-4* or *sec6-4 end4-1* cells (data not shown).

We next performed genetic crosses between the ts *mss4-102* and *sec* mutants and tested them for synthetic defects (e.g., *mss4-102* × *sec8-9* cells; Figure 1B). We found that haploid segregants bearing a *mss4-102* mutation and either *sec2-41*, *sec8-9*, *sec9-4*, *sec15-2*, *cdc42-6*, *myo2-66*, or *sac1-6* mutations resulted in lethality (Figure 1C). These synthetic interactions suggest that Mss4 is involved in secretion and that cell death may result from a combination of PI(4,5)$P_2$ production and secretory defects.

The growth deficit of *sec* mutants results from defects in vesicle transport and mutants accumulate an abnormally large intracellular pool of invertase enzyme at restrictive temperatures. To assess whether the growth enhancement seen upon *MSS4* overexpression results from the restoration of secretion, we examined invertase synthesis and secretion in *sec12-1* cells overexpressing *MSS4*. We found that defects in invertase secretion were completely rescued in *sec12-1* cells overexpressing *MSS4*, in contrast to *sec12-1* cells expressing vector alone, at restrictive temperature (Figure 1D). Importantly, *mss4-102* cells are themselves defective in invertase secretion at the restrictive temperature (Figure 1D). Together, the results imply that Mss4 regulates protein secretion.

### *MSS4 Overexpression Restores Polarized Actin in Secretory Mutants*

Mutants in the secretory pathway have severe defects in actin organization at elevated temperatures (Aronov and Gerst, 2004). Actin patches (putative sites of endocytosis) were delocalized, and actin cables absent in all mutants were examined. These defects occurred rapidly (within minutes) upon temperature shifting and did not change with time (Aronov and Gerst, 2004). Actin defects also occurred in temperature-shifted WT cells but underwent a rapid recovery in contrast to *sec* mutants (Aronov and Gerst, 2004). Because Mss4 is a regulator of the actin cytoskeleton (Audhya *et al*., 2000), we tested whether suppression of the growth defects of *sec* mutants by *MSS4* correlates with the restoration of polarized actin. Actin cables and patches were labeled using rhodamine-conjugated phalloidin (Figure 2). Actin was polarized in WT cells, however, actin cables were absent and the actin staining observed to be cytoplasmic in *mss4-102* cells, as reported previously (Desrivieres *et al*., 1998). The *cdc42-6* and *sec mutants* (i.e., *sec4-8*, *sec8-9*, *sec9-4*, and *sec15-2* cells) examined showed actin organization defects to different extents at permissive temperatures (26°C), whereas showing high levels of disorganization after the shift to restrictive temperatures (37°C for *sec* mutants; 33°C for *cdc42-6* cells) (Figure 2), as reported previously (Aronov and Gerst, 2004). Importantly, *MSS4* overexpression markedly restored the polarized organization of actin in *mss4-102*, *sec*, and *cdc42-6* yeast (Figure 2). Thus, *MSS4* overexpression [which leads to enhanced PI(4,5)$P_2$ synthesis] confers normal actin organization to mutants defective in exocytosis and actin. This reinforces the idea that a signal regulating both actin and secretion is transmitted from Mss4.

### *MSS4 Overexpression Restores Shmoo Formation in Secretory Mutants*

Another polarized growth process in *S. cerevisiae* is formation of a mating projection (shmoo) in response to pheromone signaling. In haploid cells treated with mating pheromone of the opposite mating type, polarized extensions of the cell surface occur in a manner dependent upon actin and the secretory pathway. To determine whether Mss4 activity restores shmoo formation in temperature-shifted late *sec* mutants, we overexpressed *MSS4* in WT and *sec15-2* cells and treated them with α-factor before shifting to the restrictive temperature. Treatment of *MAT*a cells with α-factor resulted in G1 arrest, followed by growth of the mating projection (data not shown; Supplemental Figure S1A). After α-factor treatment, almost all WT cells exhibited a mating projection bearing actin patches highly concentrated at the tip (Supplemental Figure S1B). Addition of α-factor to *sec15-2* cells induced formation of mating projections in 66%

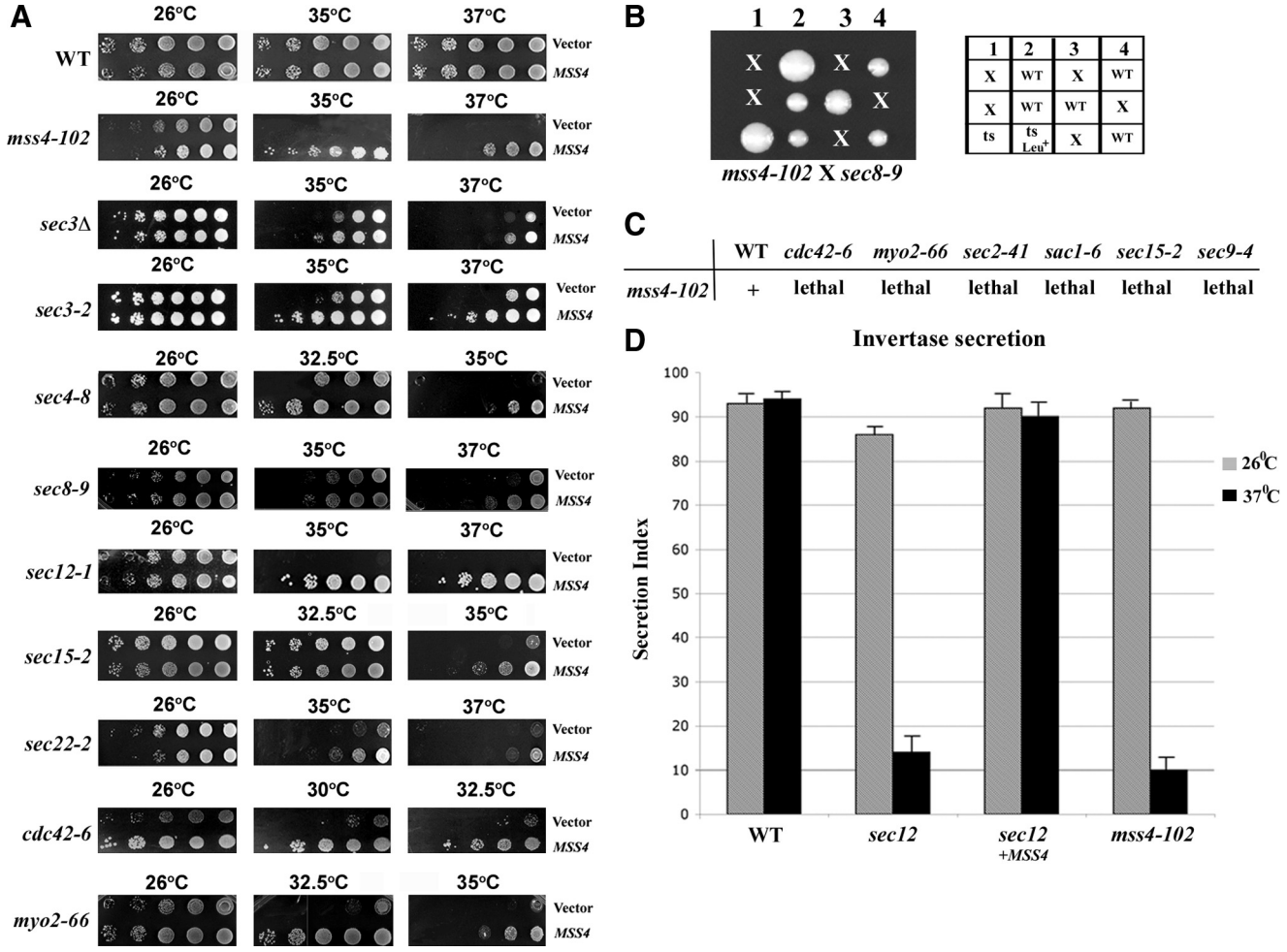


**Figure 1.** *MSS4* overexpression rescues growth and secretion defects. (A) *MSS4* overexpression suppresses growth defects. Indicated strains were transformed with control vector or vector overexpressing *MSS4* (pRS426Mss4). Cells were grown overnight, diluted serially, plated, and incubated for 48 h at the indicated temperatures (Celsius). (B) A *mss4-102* × *sec8-9* cross leads to synthetic lethality. *MAT*α *mss4-102* cells were crossed to *MAT*a *sec8-9* cells. Meiotic segregants were tested for growth at 26 and 37°C on YPD. Spores that germinated but did not form a colony are denoted with an "x" (lethality). Viable colonies were tested for ts growth and presence of the *LEU2*-linked *mss4-102* allele (*Leu*$^+$). WT indicates colonies that were not ts. (C) Mutations with defects in secretion or actin are synthetic lethal with *mss4-102*. Indicated mutants were crossed with *mss4-102* cells. Viability of the meiotic segregants and distribution of the ts and Leu$^+$ (*LEU2*) markers were examined. "+" indicates viability, whereas "lethal" indicates inviability of the double mutants on YPD at 26°C. (D) *mss4-102* cells are defective in invertase secretion and *MSS4* overexpression restores secretion in *sec12-1* cells. Invertase activity was measured in WT cells, *sec12-1* cells transformed with empty vector or pRS426Mss4, and *mss4-102* cells (lacking *SUC2*) bearing a plasmid expressing *SUC2* from a starvation-inducible promoter (pUG36Suc2). *sec12-1* and *mss4-102* cells were derepressed (2.5 h) in low-glucose medium or low-glucose medium lacking methionine, respectively. Secretion index represents the percentage of external (secreted) invertase compared with total invertase activity measured at 26 and 37°C. The representative experiment shown plots the mean of triplicate samples for each strain assayed, along with an error bar representing the SE of the mean. This experiment was repeated two additional times and gave similar results (our unpublished observations).

of the cells at the permissive temperature but in only 12% of cells at the restrictive temperature (Supplemental Figure S1A). Moreover, actin patches and cables were fully delocalized in *sec15-2* cells at the restrictive temperature (Supplemental Figure S1B).

In contrast, *MSS4* overexpression significantly improved shmoo formation in *sec15-2* cells. On *MSS4* overexpression, 38% of α-factor-treated *sec15-2* cells displayed shmooing at the restrictive temperature (Supplemental Figure S1A), whereas polarized actin was observed in 43% of cells (Supplemental Figure S1B). This indicates that Mss4 also acts downstream of the exocytic apparatus in mating factor-treated cells and rescues defects in shmooing that occur upon a block in exocytosis.

### *PI(4,5)$P_2$ Distribution Is Altered in sec Mutants and Rescued by MSS4 Overexpression*

Because *MSS4* interacts genetically with *sec* mutations, it suggests that the PI(4,5)$P_2$ pool at the PM could be altered in these cells. To detect PI(4,5)$P_2$, we used a high-affinity PI(4,5)$P_2$-specific fusion protein containing two tandem copies of the PLCδ PH domain fused to GFP [GFP-2XPH(PLCδ); Stefan *et al*., 2002)] and expressed it in WT cells and *sec* mutants (Figure 3A). In WT cells, we observed GFP-2XPH-(PLCδ) fluorescence at the PM and weakly in the cytosol, but not on intracellular compartments, as reported previously (Stefan *et al*., 2002). However, in temperature-shifted *mss4-102* cells, GFP fluorescence was diffuse throughout the cytosol (Figure 3A), indicating that GFP-2XPH(PLCδ) recruit-

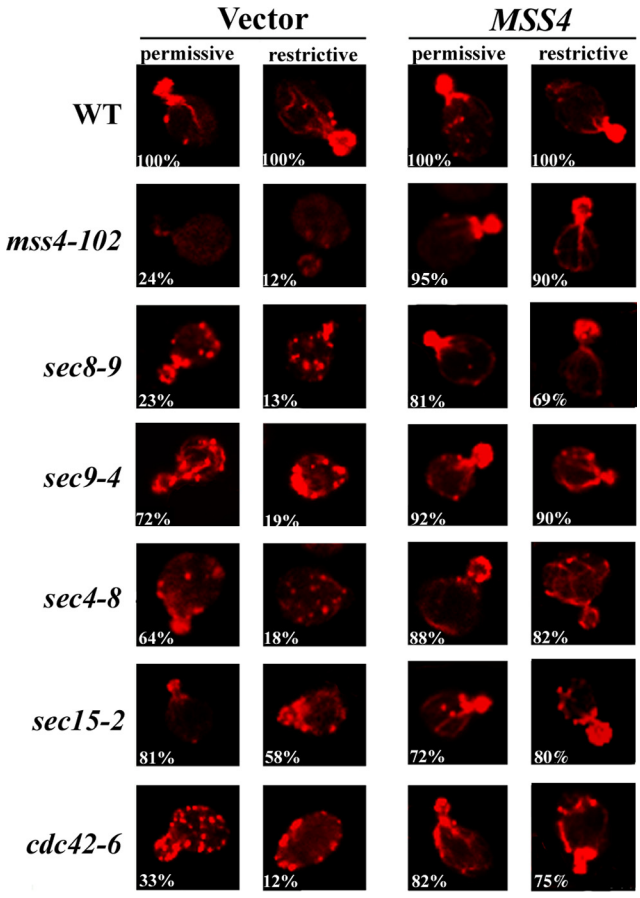


**Figure 2.** Actin delocalization in late *sec* mutants is rescued by *MSS4* overexpression. Indicated strains transformed with control vector or pRS426Mss4 were grown to log phase and either maintained at 26°C (permissive) or shifted to elevated temperatures (restrictive) for 1 h before fixation and phalloidin labeling. The restrictive temperature was 33°C for *cdc42-6* cells, whereas 37°C was used for other strains. Numbers indicate the percentage of cells, out of 100 cells examined (n = 100) for each strain, in which polarized actin was observed.

ment to the PM is dependent on Mss4 activity (Stefan *et al.*, 2002).

At permissive temperatures, GFP-2XPH(PLCδ) localized properly to the PM in *sec1-1*, *sec2-41*, *sec3*Δ, *sec3-2*, *sec4-8*, and *sec15-2* cells, as well as in *cdc42-6* cells (Figure 3A). However, GFP-2XPH(PLCδ) was mislocalized in *sec* mutants at the elevated temperature and associated with small punctate structures (Figure 3, A and B). Punctate GFP-2XPH(PLCδ) labeling was observed previously in cells lacking the yeast synaptojanins (i.e., Sjl1 and Sjl2), which dephosphorylate $PI(4,5)P_2$ (Stefan *et al.*, 2002), although labeling of the PM was not altered (data not shown). The punctate structures seen here are likely to be endosomes as they colabel with Snx4-red fluorescent protein (RFP), an endosomal marker (Hettema *et al.*, 2003), in both *sec1-1* (Figure 3C) and *sec22-2* cells (data not shown). By using an endocytosis-deficient mutation, *end4-1*, GFP-2XPH(PLCδ) was observed to remain at the PM and also localize to puncta juxtaposed with the PM, in a late *sec* mutant (Figure 3D). This indicates that $PI(4,5)P_2$ synthesized at the PM can access endosomal compartments upon a block in secretion and explains why GFP-2XPH(PLCδ) colocalizes with Snx4-containing structures. Importantly, *MSS4* overexpression restored GFP-2XPH-(PLCδ) localization to the PM in the *sec* and *cdc42-6* mutants (Figure 3B). Thus, defects in secretion affect the normal steady-state distribution of $PI(4,5)P_2$ but can be compensated for by Mss4 overproduction.

To verify that $PI(4,5)P_2$ distribution is altered in the *mss4-102* and *sec* mutants, we examined its levels in different cellular fractions using a monoclonal anti-phosphatidylinositol bisphosphate ($PIP_2$) antibody used for quantitative $PI(4,5)P_2$ detection (Hood *et al.*, 2003; Taverna *et al.*, 2007) and in situ fluorescence labeling similar to GFP-2XPH(PLCδ) (Micheva *et al.*, 2001; Faucherre *et al.*, 2005). As shown in Figure 4A, this anti-$PIP_2$ antibody recognizes only $PI(4,5)P_2$ in an array of bona fide phosphoinositide standards. To measure $PI(4,5)P_2$ levels in the *mss4-102* and *sec* mutant mutants at both permissive and restrictive temperatures, we performed subcellular fractionation by differential centrifugation to generate 10,000 × *g* and 100,000 × *g* pellet (P10 and P100, respectively) and supernatant (S10 and S100, respectively) fractions. Samples from these fractions were subjected to dot-blot analysis (Figure 4B) and quantitated vis à vis the $PI(4,5)P_2$ standard (for a representative experiment, see Figure 4C and Table 3). Total $PI(4,5)P_2$ levels were similar in cells grown at 26°C (although *mss4-102* cells had lower amounts); however, these levels declined significantly (~40%) in the mutants after the temperature shift (Table 3). Thus, temperature-sensitive $PI(4,5)P_2$ synthesis was observed in the *mss4* (as seen previously; Audhya and Emr, 2003) and *sec* mutants, and even a slight decline was observed in wild-type (WT) cells. Approximately 50% of total cellular $PI(4,5)P_2$ was found in the P100 fraction (which contains Golgi, endosomes, and secretory vesicles; Walworth *et al.*, 1989) from all strains grown at 26°C. However, the amount of $PI(4,5)P_2$ detected in the P100 declined by ~40% in the *mss4-102*, *sec4-8*, and *sec12-1* cells shifted to 37°C, to yield 27.5, 33.7, and 26.3% of the total, respectively (Table 3). Thus, the decline in $PI(4,5)P_2$ synthesis, observed at 37°C in the mutants, translates into a decrease in $PI(4,5)P_2$ levels in the P100 fraction upon the cessation of Mss4 function or a block in secretion. This decline is not likely to be connected to PI-phosphatase function, because the overexpression of *SJL1-3* in the *sec* mutants had no negative effect upon growth (data not shown).

Together, these results suggest that $PI(4,5)P_2$ is mislocalized and its levels reduced in both *mss4-102* and *sec* mutants. Because *MSS4* overexpression correlates with the restoration of normal growth, actin organization, and $PI(4,5)P_2$ localization in yeast defective in secretion, it would seem that Mss4 acts downstream of the exocytic apparatus and generates $PI(4,5)P_2$ in response to constitutive secretion.

### *Mss4 Is Localized Properly in Late Secretory Mutants*

Mss4 localization to the PM is essential for function, because *mss4-102* mutants exhibit a cytoplasmic distribution of Mss4 that is coupled with actin cytoskeleton defects (Homma *et al.*, 1998). To test whether integrity of the secretory pathway is important for Mss4 localization, we expressed Mss4-GFP from a single-copy plasmid in WT and *sec* mutant strains and examined localization. As shown in Figure 3E, Mss4-GFP localizes to the PM in both *sec* mutants and WT cells at all temperatures, suggesting that the observed defects in $PI(4,5)P_2$ distribution (Figures 3 and 4) are not due to Mss4 mislocalization but to defects in Mss4 function.

### *Cdc42 Mislocalization in Secretory Mutants Is Rescued by Mss4 Overproduction in a Cdc24-independent Manner*

The loss of polarity observed in temperature-shifted *sec* mutants might result from defects in $PI(4,5)P_2$ synthesis and

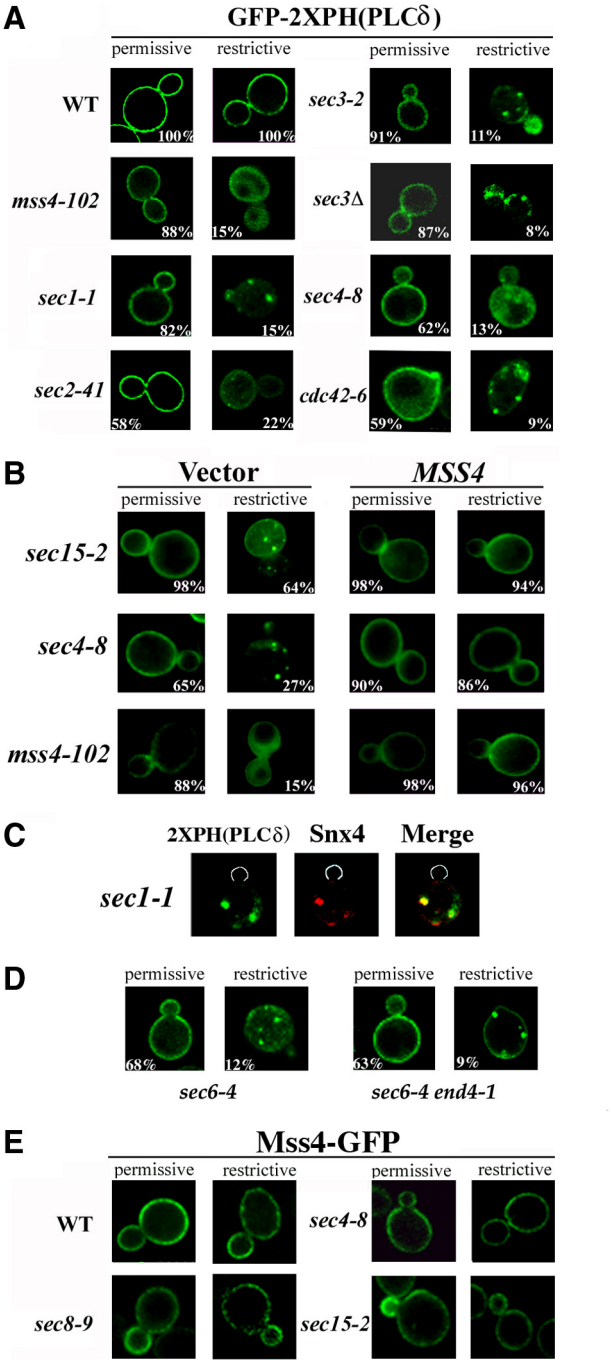


**Figure 3.** *MSS4* overexpression restores PI(4,5)$P_2$ distribution in *sec* mutants. (A) PI(4,5)$P_2$ distribution is altered in the *sec* and *cdc42-6* mutants. The indicated strains were transformed with a vector expressing GFP-2XPH(PLCδ) (pRS426GFP-2XPH(PLCδ)) and maintained at 26°C or shifted for 1 h at 37°C. Numbers indicate the percentage of cells in which PM localization of GFP-2XPH(PLCδ) was observed (n = 100 cells counted). (B) *MSS4* overexpression restores normal PI(4,5)$P_2$ distribution to the PM. The indicated strains were cotransformed with pRS426GFP-2XPH(PLCδ) and either a control vector or vector expressing *MSS4* (pAD54Mss4). Cells were maintained at 26°C or shifted for 1 h to 37°C before visualization. Numbers indicate the percentage of cells in which PM localization of GFP-2XPH(PLCδ) was observed (n = 100 cells counted). (C) PI(4,5)$P_2$ accumulates in endosomes upon blockage of the secretory pathway. *sec1-1* cells expressing GFP-2XPH(PLCδ) and RFP-Snx4 (pAD54-RFP-Snx4) were grown at 26°C and shifted for 1 h to 37°C, before visualization. (D) PI(4,5)$P_2$ accumulation in endosomes is dependent on endocytosis. *sec6-4* and *sec6-4 end4-1* cells expressing GFP-2XPH(PLCδ) were grown at 26°C and shifted for 1 h to 37°C, before visualization. (E) Mss4 localization is not altered in late *sec* mutants. Indicated strains were transformed with pUG35Mss4-GFP. Cells were induced in medium lacking methionine for 1 h and maintained at 26°C or shifted to 37°C for 1 h before visualization.

signaling to downstream effectors. To test this, we examined localization of the Cdc42 GTPase, which is involved in actin regulation and polarity establishment (Etienne-Manneville, 2004; Irazoqui and Lew, 2004; Pruyne *et al*., 2004), in late *sec* mutants. Cdc42 localizes to the cell periphery and vacuolar limiting membrane; however, during budding it concentrates at the incipient bud site and the newly forming bud (Richman *et al*., 2002). To determine whether defects in exocytosis or PI(4,5)$P_2$ production alter Cdc42 localization, we examined the localization of RFP-Cdc42 in WT, *mss4-102*, and *sec* mutants at permissive and restrictive temperatures. As seen in Figure 5A, RFP-Cdc42 localized both to the PM and vacuolar limiting membrane, and concentrated in the small buds of WT cells, as reported previously (Richman *et al*., 2002). We verified RFP-Cdc42 localization also to the vacuolar limiting membrane of WT cells by using GFP-tagged Vph1 (data not shown). In contrast, RFP-Cdc42 was mislocalized in *mss4-102* cells and both *sec4-8* and *sec15-2* cells at permissive temperatures, being present in the cytoplasm and in what seem to be internal membranes (Figure 5A). The aberrant localization of RFP-Cdc42 was further exacerbated upon the shift to restrictive temperatures, particularly in *sec15-2* cells, and seemed to be possibly cytosolic (Figure 5A). However, *MSS4* overexpression restored the normal localization of RFP-Cdc42 in both the *mss4-102* and *sec* mutants (Figure 5A).

We verified the restoration of Cdc42 localization by Mss4, as seen in Figure 5A, by using cell fractionation (Figure 5B). We expressed GFP-tagged Cdc42 from a single-copy plasmid in WT, *mss4-102*, and *sec4-8* cells and examined its distribution to the S10/P10 and S100/P100 fractions. Interestingly, we noted that Cdc42 levels declined significantly in the *mss4-102* cells, especially at the restrictive temperature. In contrast, the levels of a control plasma membrane protein, Sso1/2, were unaffected. This may indicate that mislocalized Cdc42 (observed in the *mss4-102* and *sec* cells; Figure 5A) undergoes enhanced degradation. In fractions derived from WT cells, Cdc42 was present primarily in the endoplasmic reticulum (ER)- and PM-containing P10 fraction, but also in the P100 fraction, which typically contains endosomes and vesicles. This same pattern was basically observed in *mss4-102* and *sec4-8* cells at 26°C. However, Cdc42 was found only in the P10 in *sec4-8* cells shifted to 37°C (Figure 5B), indicating that the protein is probably not cytosolic even when mislocalized. In contrast, *MSS4* overexpression in *sec4-8* cells resulted in both elevated levels of Cdc42 protein and restoration of its distribution to the P10 fraction. Thus, the restoration of Cdc42 localization by Mss4 overproduction (Figure 5A) correlates with its normal subcellular distribution (Figure 5B). Overall, Mss4-mediated rescue of the late *sec* mutants (Figure 1A) is concomitant with the restoration of PI(4,5)$P_2$ levels (Figures 3 and 4), Cdc42 localization (Figure 5, A and B), and polarization of the actin cytoskeleton (Figure 2).

Because actin regulation by PI(4,5)$P_2$ signaling and Cdc42 are tightly connected (Yin and Janmey, 2003; Irazoqui and Lew, 2004; Pruyne *et al*., 2004; Levin, 2005; Strahl and Thorner, 2007), we hypothesized that *CDC42* overexpression should

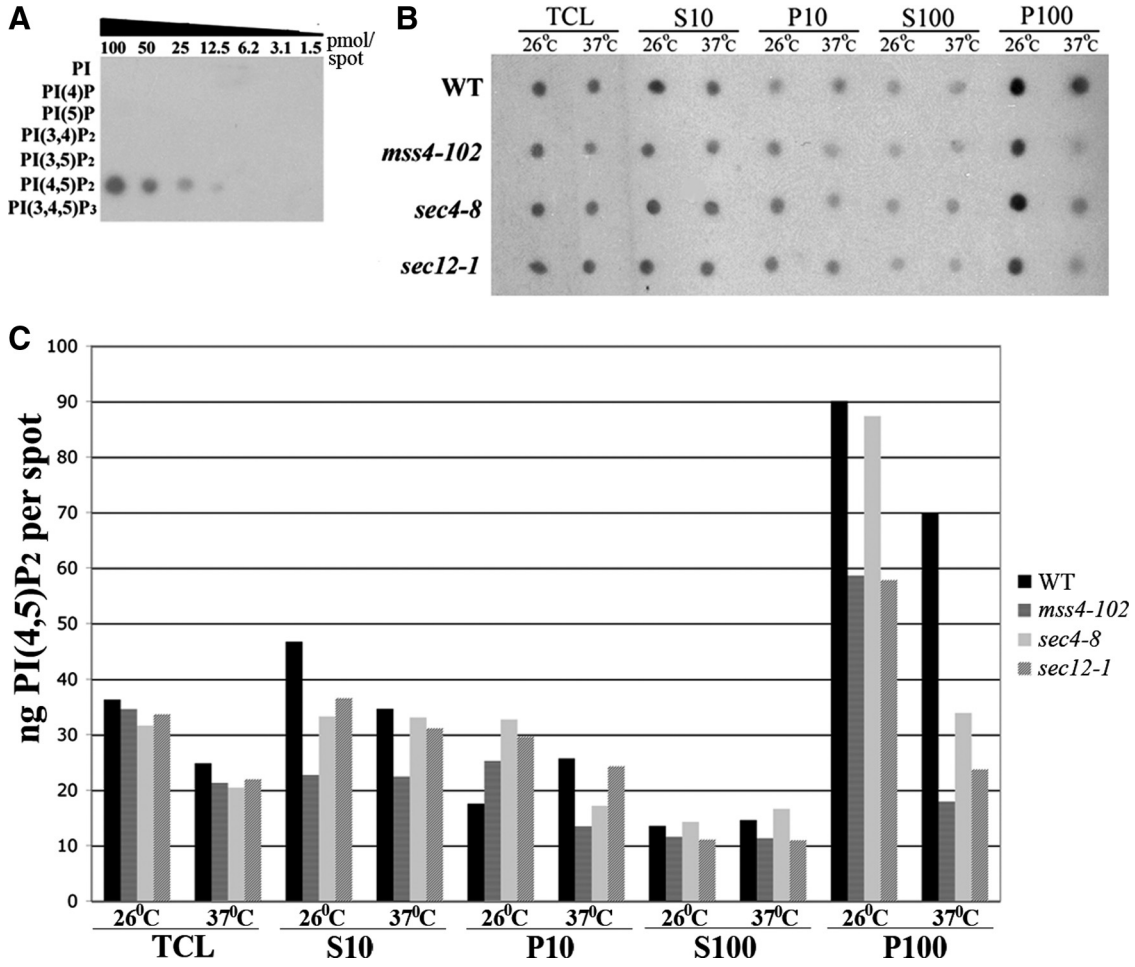


**Figure 4.** PI(4,5)$P_2$ levels are altered in *mss4-102* and *sec* mutants. (A) Specificity of anti-$PIP_2$ antibodies. An array containing decreasing concentrations of phosphoinositide standards, as indicated, was probed with an anti-$PIP_2$ antibody (1:5000). (B) Subcellular fractionation of PI(4,5)$P_2$. The indicated strains were grown to mid-log phase and either maintained at 26°C or shifted for 1 h to 37°C and processed for cell fractionation (see *Materials and Methods*). Samples (0.5 $\mu$g of protein) from all fractions (S10, P10, S100, and P100) and TCLs were subjected to dot-blot analysis by using the anti-$PIP_2$ antibody (1:5000). (C) Quantification of PI(4,5)$P_2$. Densitometry was used to quantify PI(4,5)$P_2$ in the different fractions, relative to the standard curve generated from A. Optical densities were measured and normalized for background, by using Image-Gauge software (Fujifilm). The amount of $PIP_2$ present per 0.5 $\mu$g of protein for each fraction is graphed. A representative experiment out of three individual experiments having similar results is shown.

rescue the growth of *mss4-102* cells, as well as late *sec* mutants. As shown in Figure 5C, *CDC42* overexpression rescued the growth defects of *mss4-102* cells at all temperatures. Correspondingly, *MSS4* overexpression rescued the temper-

**Table 3.** Distribution of PI(4,5)$P_2$ in cell fractions

| | % of total PI(4,5)$P_2$ | | | | | | | |
|---|---|---|---|---|---|---|---|---|
| | WT strain | | *mss4-102 strain* | | *sec4-8 strain* | | *sec12-1 strain* | |
| | 26°C | 37°C | 26°C | 37°C | 26°C | 37°C | 26°C | 37°C |
| Fraction | | | | | | | | |
| S10 | 27.8 | 23.9 | 19.2 | 34.4 | 19.8 | 32.8 | 27 | 34.5 |
| P10 | 10.5 | 17.7 | 21.3 | 20.7 | 19.5 | 17 | 22 | 27 |
| S100 | 8 | 10 | 9.7 | 17.3 | 8.5 | 16.5 | 8 | 12.1 |
| P100 | 53.7 | 48.3 | 50 | 27.5 | 52.2 | 33.7 | 42.8 | 26.3 |
| Total $PIP_2$ (ng/2 $\mu$g protein) | 167.7 | 144.6 | 117.8 | 64.7 | 167.5 | 100 | 135 | 90 |
| $\Delta$ in P100 (%) (37°C/26°C) | −10 | | −44.6 | | −35.3 | | −38.4 | |
| $\Delta$ in total $PIP_2$ level (%) | −13.8 | | −45 | | −40 | | −33.4 | |

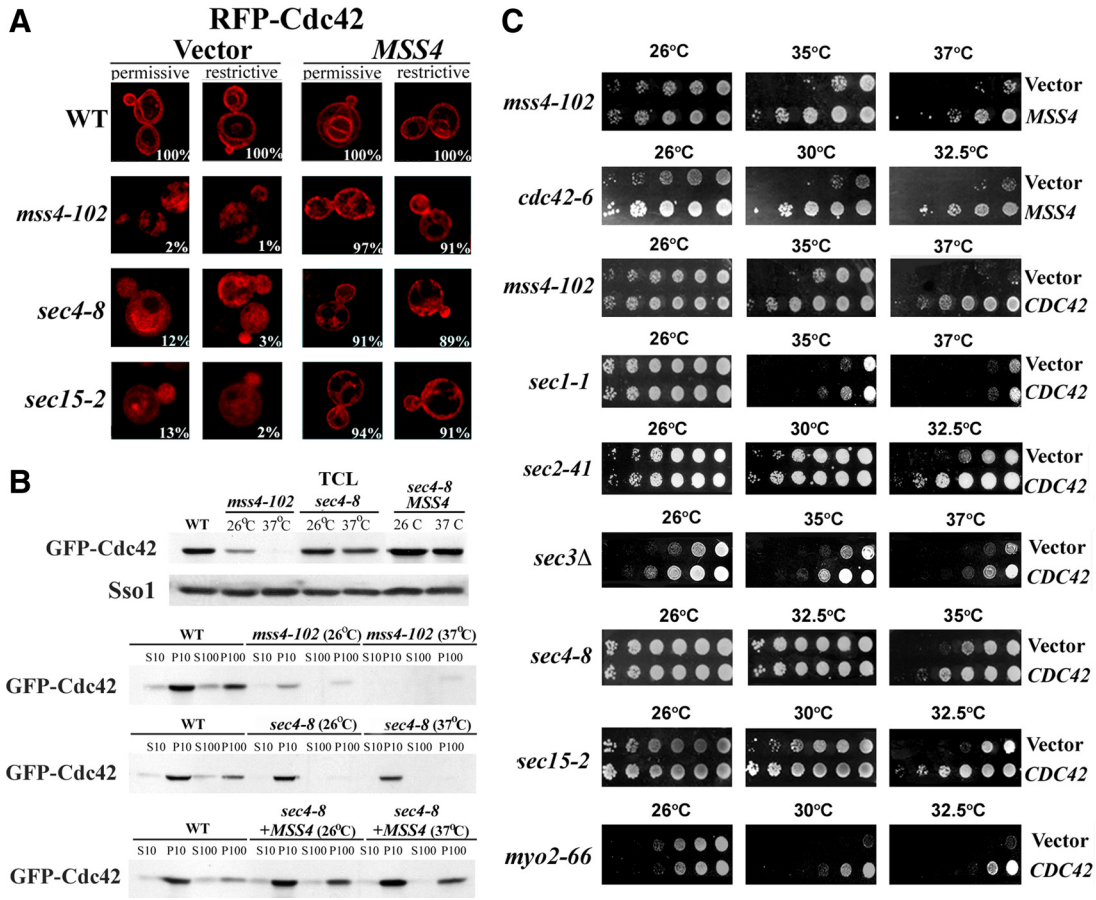


**Figure 5.** Cdc42 localization is impaired in *sec* mutants and restored by *MSS4* overexpression. (A) RFP-Cdc42 is mislocalized in the *mss4-102* and *sec* mutants. The indicated strains were cotransformed with pAD54-RFP-Cdc42, which expresses RFP-Cdc42, and either a control vector or pRS426Mss4. Cells were maintained at 26°C or shifted for 1 h to 37°C before visualization. Numbers indicate the percentage of cells in which normal PM and vacuolar localization of RFP-Cdc42 was observed (n = 100 cells counted). (B) Subcellular fractionation of GFP-Cdc42. WT, *mss4-102*, and *sec4-8* cells cotransformed with GFP-Cdc42 (pUG36GFP-Cdc42) and either a control vector or pGBKMss4 (+*MSS4*) and were grown to mid-log phase in medium lacking methionine. Cells were either maintained at 26°C or shifted for 1.5 h to 35°C and then lysed. Lysates were subjected to differential centrifugation to obtain the P10, S10, P100, and S100 fractions (see *Materials and Methods*). Samples of the fractions and TCLs were resolved by SDS-PAGE and detected in blots using anti-GFP and -Sso1 antibodies. (C) *CDC42* overexpression enhances the growth of *mss4-102*, *cdc42-6*, and late *sec* mutants. *mss4-102* cells were transformed either with control vector or pRS426Mss4 (uppermost row). Other *mss4-102* cells were transformed with control vector or pUG36GFP-Cdc42 (third row from top). *cdc42-6* cells were transformed with control vector or pRS426Mss4 (second row from top). Late *sec* mutants *sec1-1*, *sec2-41*, *sec3*Δ, *sec4-8*, *sec15-2*, and *myo2-66* were transformed with control vector or pUG36GFP-Cdc42. Cells were grown in selective medium or medium lacking methionine, diluted serially, plated, and incubated for 48 h at the indicated temperatures (Celsius).

ature-sensitive growth defects of *cdc42-6* cells at all temperatures. Thus, both Mss4 and Cdc42 overproduction effect the same cellular response. Next, we examined genetic interactions between *CDC42* and the late *sec* mutants. We found that *CDC42* overexpression ameliorated the growth of late *sec mutants* (e.g., *sec1-1*, *sec2-41*, *sec3*Δ, *sec4-8*, *sec15-2*, and *myo2-66*) cells at semirestrictive and restrictive temperatures. Together, these experiments suggest that Mss4 acts as the transducer of an exocytic signal leading from the secretory apparatus to the actin cytoskeleton via Cdc42.

To elucidate how the exocytic signal is transmitted from Mss4 to Cdc42, we investigated whether Cdc24, a Cdc42 GEF that contains a potential PI(4,5)$P_2$-binding PH domain, is involved. Cdc24 localizes to sites of polarized growth and is essential for actin polarization (Toenjes *et al*., 1999). Cdc24-GFP was inducibly expressed from a single-copy plasmid and localized to the bud tips of WT cells at all temperatures, and to what may be the nucleus in *mss4-102* cells at 35°C (Supplemental Figure S2A). The localization of Cdc24 to the nucleus before division has been described previously (Toenjes *et al*., 1999). Cdc24-GFP localization was normal in the *sec8-9* and *sec15-2* cells at 35°C but became mislocalized to small punctate structures in the cytoplasm at 37°C. However, *MSS4* overexpression failed to restore the normal localization of Cdc24-GFP in the *sec* mutants at 37°C. This indicates that another component, aside from PI(4,5)$P_2$, regulates Cdc24 localization in cells defective in exocytosis.

Supportive of the idea that Mss4 and Cdc24 act independently, we found that *MSS4* overexpression failed to suppress the growth defects of *cdc24-1* cells, whereas *CDC24* overexpression failed to suppress the growth defects of *mss4-102* cells (Supplemental Figure S2B). Moreover, PI(4,5)$P_2$ distribution was normal in *cdc24-1* cells, as assessed by GFP-2XPH(PLCδ) localization (Supplemental Figure S2C). Thus, Cdc24 does not mediate the exocytic signal connecting Mss4 to Cdc42 and actin regulation.

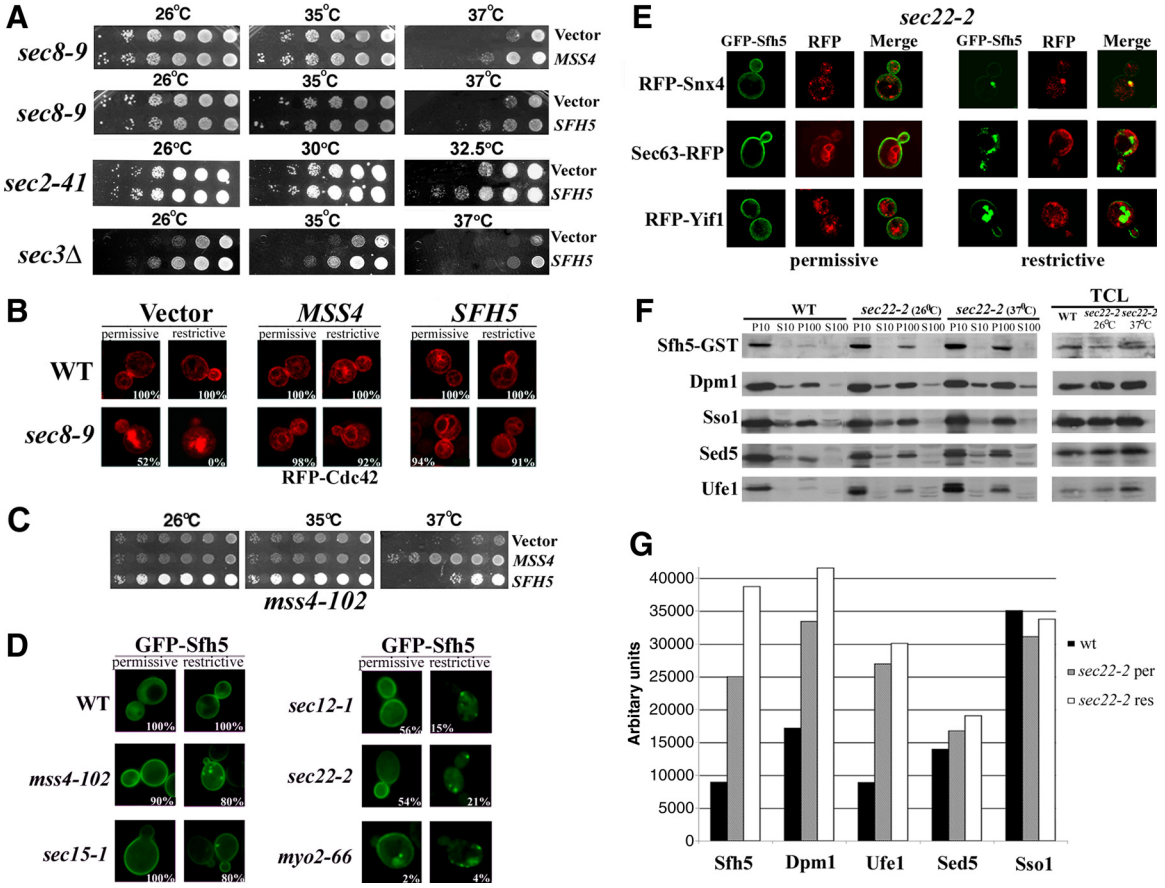


**Figure 6.** Sfh5 acts with Mss4 to transduce the exocytic signal to Cdc42. (A) *SFH5* overexpression rescues late *sec* mutants. Top, *sec8-9* cells were transformed with control vector or pRS426Mss4. Second to fourth panels, *sec8-9*, *sec2-41*, and *sec3*Δ cells were transformed either with control vector or pRS426Sfh5 (*SFH5*). Cells were grown overnight, diluted serially, plated, and incubated for 48 h at the indicated temperatures (Celsius). (B) RFP-Cdc42 mislocalization in *sec8-9* cells is rescued by *SFH5* overexpression. The indicated strains were cotransformed with pAD54-RFP-Cdc42 and control vector, pRS426Mss4 (*MSS4*), or pRS426Sfh5 (*SFH5*). Cells were maintained at 26°C or shifted for 1 h to 37°C before visualization. (C) *SFH5* overexpression enhances the growth of *mss4-102* cells. *mss4-102* cells were transformed with control vector, pUG35Mss4-GFP, or pUG36GFP-Sfh5. Cells were grown in medium lacking methionine, diluted serially, plated, and incubated for 48 h at the indicated temperatures (Celsius). (D) GFP-Sfh5 is mislocalized in *sec* mutants. The indicated strains were transformed with pUG36GFP-Sfh5, grown in medium lacking methionine (1 h), and either maintained at 26°C or shifted for 1 h to 37°C, before visualization. Numbers indicate the percentage of cells in which PM localization of GFP-Sfh5 was observed (n = 100 cells counted). (E) Sfh5 and Snx4 colocalize at endosomal compartments. *sec22-2* cells were cotransformed with pUG36GFP-Sfh5 and either pAD54-RFP-Snx4, pSM1960-Sec63-RFP, or pAD54-RFP-Yif1. Cells were grown in medium lacking methionine (1 h) and either maintained at 26°C or shifted for 1 h to 37°C, before visualization. (F) Subcellular fractionation of Sfh5. WT and *sec22-2* cells overexpressing GST-Sfh5 (BG1805Sfh5) were grown to mid-log phase, maintained at 26°C or shifted for 1 h to 37°C, and lysed. Lysates were subjected to differential centrifugation to obtain P10, S10, P100, and S100 fractions (see *Materials and Methods*). Samples of the fractions and TCLs were resolved by SDS-PAGE and detected in blots using anti-GST, -Dpm1, -Sso1, -Sed5, and -Ufe1 antibodies. (G) Quantification of the subcellular distribution of Sfh5. Densitometry was used to quantify the relative amounts of Sfh5 and detected markers in the P100 fraction, after normalization for protein expression. Measurements are expressed in arbitrary units. A representative experiment out of three experiments having similar results is shown.

### *Sfh5 Acts Upstream of Mss4 in Transducing the Exocytic Signal to Actin*

Genetic evidence supports a connection between exocyst function and phosphoinositides generated via the Stt4 PI 4-kinase pathway (Routt *et al.*, 2005). *SFH5*, a member of the Sec14-like PITP family that stimulates Stt4-dependent phosphoinositide synthesis in vivo, was identified as a suppressor of mutations in exocyst components (i.e., *sec8-9*) (Routt *et al.*, 2005). Furthermore, *SFH5* overexpression rescued actin defects in a Sec14-bypass mutant and was suggested to enhance Mss4-mediated PI(4,5)$P_2$ synthesis (Routt *et al.*, 2005). To investigate whether Sfh5 plays a role in conferring the exocytic signal, we expressed *SFH5* from a multi-copy plasmid in various *sec* mutants. *SFH5* overexpression ameliorated the growth of *sec2-41*, *sec3*Δ, and *sec8-9* cells and in a manner identical to *MSS4* overexpression (Figure 6A; our unpublished data).

Next, we examined RFP-Cdc42 localization in *sec8-9* cells with or without the overexpression of *MSS4* or *SFH5*. As seen in Figure 6B, RFP-Cdc42 was mislocalized in *sec8-9* cells at both temperatures. However, upon *MSS4* or *SFH5* overexpression, RFP-Cdc42 localized to the PM and vacuolar limiting membrane as in WT cells. Thus, Sfh5 acts like Mss4 in terms of its ability to restore Cdc42 localization and cell growth in exocytosis-deficient yeast.

To examine whether *MSS4* and *SFH5* interact genetically, we expressed *SFH5* inducibly from a single-copy plasmid in *mss4-102* cells. As seen in Figure 6C, *SFH5* overexpression

significantly improved the growth of *mss4-102* cells at permissive and semipermissive temperatures and even allowed them to form larger colonies than cells overexpressing *MSS4*. Thus, Sfh5 function may potentiate activity of the mutant PI(4)P 5-kinase, probably by delivering additional PI to the PM. In contrast, Sfh5 cannot replace Mss4 at the restrictive temperature, leading to growth defects (Figure 6C).

Next, we expressed GFP-Sfh5 from a single-copy plasmid to determine Sfh5 localization in the *sec* mutants. Previous findings suggested that Sfh5-GFP localizes to both the cytosol and to the PM in WT cells (Schnabl *et al*., 2003). However, studies using Sfh5-3xmyc expression in *stt4-4* cells and fluorescence imaging in situ suggest a pattern of labeling that might include ER peripheral to the PM (Routt *et al*., 2005; Mousley *et al*., 2006). These studies used chromosomal integration and expression to examine Sfh5 localization; however, this method of genome tagging invariably disconnects the 3′ untranslated region (UTR) of *SFH5* from its open reading frame. Because removal of the 3′UTR affects the localization of nonanchored polarity and secretion factors, such as Sro7 (Aronov *et al*., 2007), we examined the localization of GFP-Sfh5 expressed under an inducible promoter and bearing its 3′UTR. GFP-Sfh5 localized to the cytosol and PM in WT cells (Figure 6D), whereas it localized to the PM and numerous small punctate structures in *mss4-102* and *sec15-1* cells at the restrictive temperature (Figure 6D). Importantly, GFP-Sfh5 was absent from the PM and localized only to intracellular structures in mutants of the early secretory pathway (i.e., *sec22-2*, *sec12-1* cells), as well as in the *myo2-66* cells at restrictive temperatures (Figure 6D). Because *MYO2* encodes a myosin responsible for the transport of secretory vesicles along actin cables (Irazoqui and Lew, 2004; Pruyne *et al*., 2004), it suggests that Sfh5 delivery to the PM is actin- and myosin-dependent.

Because the punctate structures labeled by GFP-Sfh5 are similar in appearance to endosomes, we examined whether GFP-Sfh5 colocalizes with Snx4-RFP in WT and *sec22-2* cells at both permissive and restrictive temperatures (Figure 6E). We found that GFP-Sfh5 and Snx4-RFP colocalized to the same punctate structures in *sec22-2* cells. 4,6-Diamidino-2-phenylindole staining verified that these structures were nonnuclear (data not shown). Experiments employing Sec63-RFP or RFP-Yif1 revealed that the Sfh5-containing structures seen at restrictive temperatures in *sec22-2* cells do not colocalize with either the ER or Golgi, respectively (Figure 6E). This indicates that Sfh5 accumulates at endosomes upon an inhibition in ER–Golgi transport. Thus, Sfh5 is transported to the PM in a Myo2-dependent manner (Figure 6D) and, upon a block in the secretory pathway, accumulates at endosomal structures (Figure 6E).

To verify the change in the subcellular distribution of GFP-Sfh5 upon a block in the secretion, we overexpressed GST-Sfh5 in WT and *sec22-2* cells, and performed subcellular fractionation. To determine the intracellular distribution of GST-Sfh5, fractions were resolved by SDS-PAGE and immunoblotted with anti-GST antibodies. Sfh5, which localizes mainly to the PM (Figure 6, D and E; Schnabl *et al*., 2003) and, perhaps, the to peripheral ER (Routt *et al*., 2005; Mousley *et al*., 2006) was detected primarily in the PM- and ER-containing P10 fraction derived from WT cells. In contrast, a significant amount of Sfh5 was detected in the P100 fraction derived from *sec22-2* cells grown at 26°C, which increased significantly in cells shifted to 37°C (Figure 6F). This pattern of Sfh5 distribution was similar to that of other ER markers (i.e., Dpm and Ufe1). By using densitometry and normalizing for expression, Dpm1 and Ufe1 were found to be more abundant in the P100 fraction derived from *sec22-2* cells shifted to the restrictive temperature (Figure 6, F and G). In contrast, Sso1, a PM marker, was detected in both the P10 and P100 fractions from WT and *sec22-2* cells (Figure 6, F and G) but did not show temperature-dependent enrichment to the P100 (Figure 6, F and G). Similar results were obtained with Sed5, a *cis*-Golgi marker (Figure 6, F and G).

Together, the fluorescence microscopy and cell fractionation data imply that Sfh5 localizes to the PM, as suggested previously (Schnabl *et al*., 2003), but is trafficked to the PM from earlier compartments in an actin/myosin- and secretory pathway-dependent manner. This supports the idea that Sfh5 mediates PI delivery from the ER to the PM, as proposed previously (Routt *et al*., 2005; Mousley *et al*., 2006).

### *Mutation of the Conserved PI-binding Site in Sfh5*

The C-terminal region of Sfh proteins is highly homologous to that of Sec14 (Li *et al*., 2000; Figure 7A), which exhibits PI transfer activities (Phillips *et al*., 1999). Within this region amino acids E207 and K239 of Sec14 are highly conserved in all Sec14 homologues and mutation of K239 in Sec14 (analogous to K236 in Sfh5) blocks PI transfer activity in vitro (Phillips *et al*., 1999). Residue E207 in Sec14 (E204 in Sfh5) forms a salt-bridge with K239 and the electrostatic interaction between the E207 and K239 side chains is critical for Sec14 to bind PI (Sha *et al*., 1998). To determine whether the PI binding activity of Sfh5 is critical for its function in delivering the exocytic signal, we mutated E204 or both E204 and K236 of Sfh5 to alanine and created single-copy plasmids inducibly expressing *SFH5* $^{E204}$ or *SFH5*$^{E204A,K236A}$. As seen in Figure 7B, overexpression of *SFH5* $^{E204A}$ was less able than native *SFH5* to enhance the growth of *mss4-102* cells at elevated temperatures. Moreover, the removal of both E204 and K236 in Sfh5 resulted in a loss of function and could not rescue the growth of *mss4-102* cells (Figure 7B).

Because *SFH5* overexpression restored the normal intracellular localization of RFP-Cdc42 in *sec8-9* cells (Figure 6B), we examined the effect of *GFP-SFH5*$^{E204A,K236A}$ overexpression on Cdc42 localization (Figure 7C). Importantly, we found that RFP-Cdc42 was severely mislocalized in both WT and *sec8-9* cells expressing the mutant protein and accumulated in vacuolar compartments, as revealed by *N*-[3-triethylammoniumpropyl]-4-[*p*-diethylaminophenylhexatrienyl] pyridinium dibromide (FM4-64) labeling (Figure 7C; our unpublished observations). Thus, *SFH5*$^{E204A,K236A}$ seems to have a dominant-negative effect upon Cdc42 localization.

Finally, we examined the localization of GFP-tagged Sfh5$^{E204A,K236A}$ (Figure 7D). Unlike GFP-Sfh5, GFP-Sfh5$^{E204A,K236A}$ was found to be unable to localize at the PM in either WT or *sec8-9* cells at either 26 or 37°C. Moreover, the mislocalization of GFP-Sfh5$^{E204A,K236A}$ was further exacerbated in *sec8-9* cells at the restrictive temperature and yielded prominent large puncta (Figure 7D). Because the expression levels of GFP-Sfh5 and GFP-Sfh5$^{E204A,K236A}$ were similar (Figure 7E), these puncta and the effects of GFP-Sfh5$^{E204A,K236A}$ upon Cdc42 localization (Figure 7C) or *mss4-102* cell growth (Figure 7B) are probably not due to differences in protein levels.

## DISCUSSION

Actin undergoes rapid depolarization in *sec* mutants shifted to restrictive temperatures (Aronov and Gerst, 2004), suggesting that a relationship exists between integrity of the secretory pathway and the actin cytoskeleton. Here, we propose that a signal sent to maintain actin polarization (during secretion) is generated by vesicle- and nonclassical PITP-mediated PI delivery to the PM, resulting in PI(4,5)$P_2$

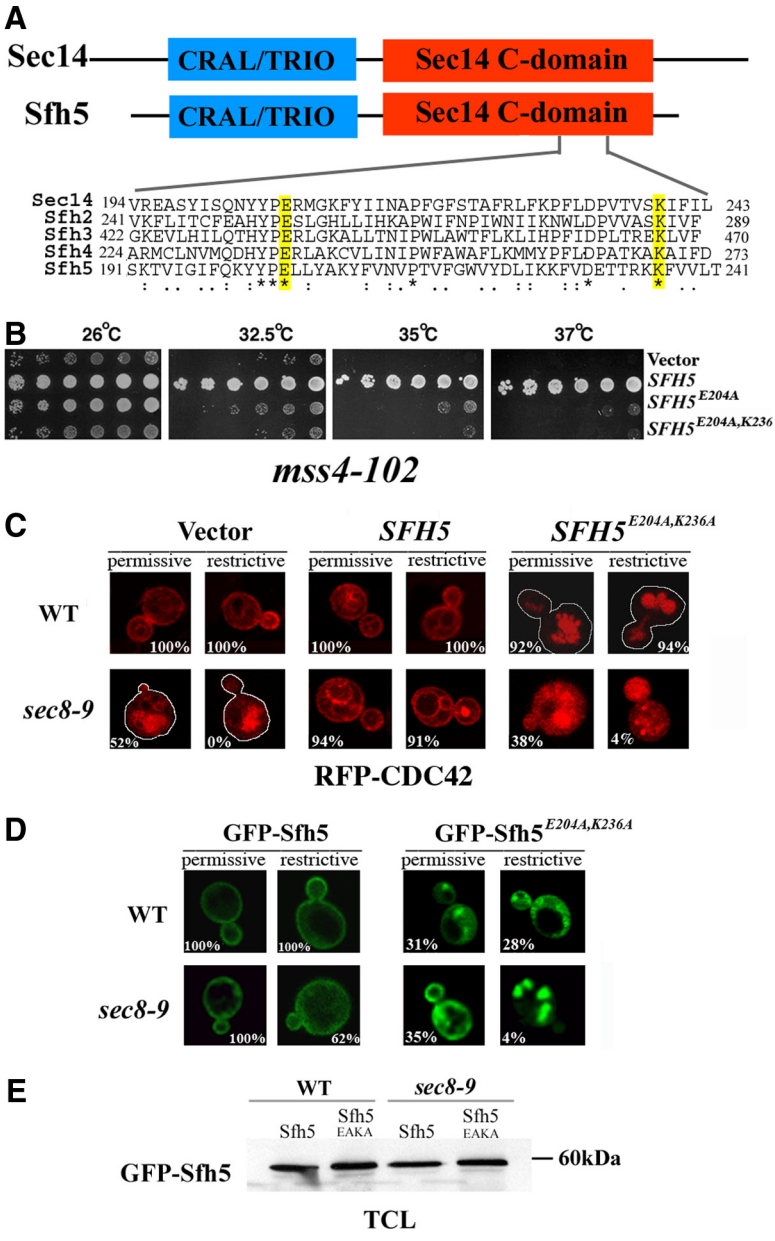


**Figure 7.** PI binding is essential for Sfh5 to transduce the exocytic signal to Cdc42 via Mss4. (A) Alignment of the C-terminals of Sec14 and Sfh2-5. Sec14 and Sfh2-5 were aligned using the ClustW algorithm. Asterisks (*) indicate conserved residues, whereas colons (:) and periods (.) indicate strongly and loosely homologous residues, respectively. Numbers indicate amino acid residues. (B) $SFH5^{E204A,K236A}$ overexpression fails to rescue the *mss4-102* mutant. *mss4-102* cells were transformed with control vector, pUG36GFP-Sfh5, pUG36GFP-$Sfh5^{K236A}$, or pUG36GFP-$Sfh5^{E204A,K236A}$. Cells were grown overnight in medium lacking methionine, diluted serially, plated, and incubated for 48 h at the indicated temperatures (Celsius). (C) $SFH5^{E204A,K236A}$ overexpression results in mislocalization of RFP-Cdc42 in WT and *sec8-9* cells. WT and *sec8-9* cells were cotransformed with pAD54-RFP-Cdc42 and either control vector, pUG36GFP-Sfh5 (*SFH5*), or pUG36GFP-$Sfh5^{E204A,K236A}$ ($SFH5^{E204A,K236A}$). Cells were grown in medium lacking methionine (1 h) and maintained at 26°C or shifted for 1 h to 37°C before visualization. The white tracings indicate the outline of the cells. (D) GFP-$Sfh5^{E204A,K236A}$ is mislocalized in WT and *sec8-9* cells. WT and *sec8-9* strains were transformed with pUG36GFP-$Sfh5^{E204A,K236A}$. Cells were grown in medium lacking methionine (1 h) and either maintained at 26°C or shifted for 1 h to 37°C, before visualization. Numbers indicate the percentage of cells in which PM localization was observed (n = 100 cells counted). (E) Expression levels of Sfh5 and $Sfh5^{E204A,K236A}$. WT and *sec8-9* cells transformed either with plasmid pUG36GFP-Sfh5 (Sfh5) or pUG36GFP-$Sfh5^{E204A,K236A}$ ($Sfh5^{EAKA}$) were grown to mid-log phase in medium lacking methionine. Cells (20 $OD_{600}$ units) were collected and lysed. Equal samples of 20 $\mu$g of the TCLs were resolved by SDS-PAGE, and Sfh5 was detected in the blot using anti-GFP (1:1000) antibodies.

synthesis by the PI kinases (Stt4 and Mss4) and PI(4,5)$P_2$-dependent regulation of actin organization via Cdc42, a regulator of actin filament formation (Figure 8). This PI(4,5)$P_2$-based "exocytic" signal is blocked upon a cessation of vesicle transport or fusion in temperature-shifted *sec* mutants and leads to cytoskeletal defects that affect polarity establishment and growth.

We base this on the following evidence. First, *MSS4* overexpression suppressed growth defects in all *sec* mutants tested by us (Figures 1A, 5B, and 6A) and others (Routt *et al.*, 2005) and restored invertase secretion to an early *sec* mutant (Figure 1D). Moreover, a mutation in *MSS4* results in secretion defects identical to *sec* mutants (Figure 1D) and is synthetic lethal in combination with *sec* mutations (Figure 1, B and C). This implies that Mss4 acts at the end of the secretory pathway. Second, there is a link between integrity of the secretory pathway and PI(4,5)$P_2$ production/localization at the PM, because a PI(4,5)$P_2$ reporter accumulates in the endosomes of *sec* mutants in an endocytosis-dependent manner (Figure 3, A–D). These changes in PI(4,5)$P_2$ levels/localization in the *mss4* and *sec* mutants were validated by quantitative analysis using a specific anti-PI(4,5)$P_2$ antibody (Figure 4 and Table 3). Third, Mss4 function connects exocytosis to actin regulation, because *MSS4* overexpression rescued defects in actin observed in *sec* mutants during budding and the mating response (Figure 2 and Supplemental Figure S1). Fourth, RFP-Cdc42 is systematically mislocalized in secretion mutants (Figures 5A, 5B, 6B, and 7C), and *MSS4* overexpression restores normal Cdc42 localization (Figures 5, A and B, and 6B). The signal propagated by Mss4 [via PI(4,5)$P_2$] is transduced to actin by Cdc42, as *CDC42* overexpression rescues *mss4* and many *sec* mutants (Figure 5C), although we cannot rule out the participation of other proteins activated by PI(4,5)$P_2$ generation. Fifth, a nonclassical PITP, Sfh5, is involved in this cascade because *SFH5* overexpression ameliorated the growth of *mss4* and *sec* mutants (Figure 6, A and C, and 7B), restored Cdc42 localization (Figures 6B and 7C), and mutations in the PI-binding do-

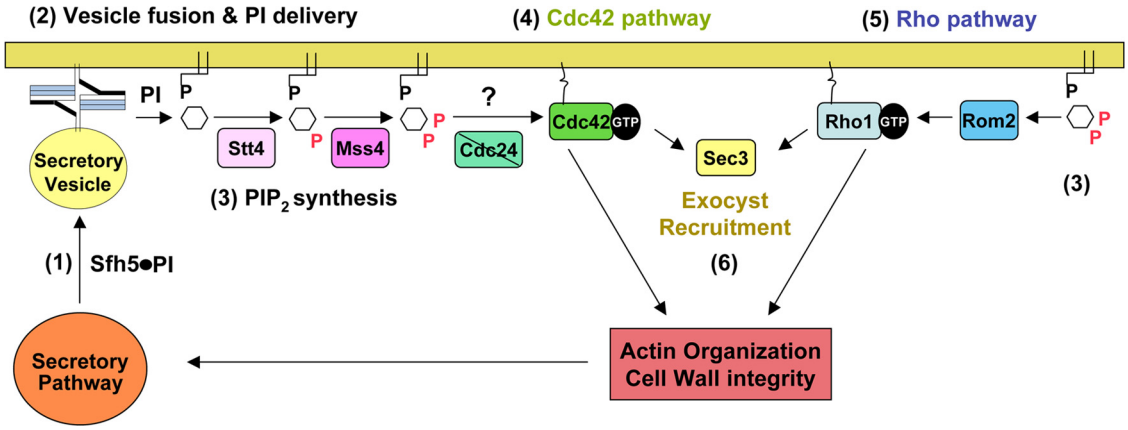


**Figure 8.** The exocytic signal conferred by PI signaling and regulation of the actin cytoskeleton. Sfh5, a nonclassical PITP, delivers PI to the PM via the (actin- and myosin-dependent) secretory pathway (1). Upon SNARE-mediated vesicle fusion at the PM (2), Sfh5 delivers PI to the PI 4-kinase and PI(4)P 5-kinase (e.g., Stt4 and Mss4) to generate $PI(4,5)P_2$ (3). $PI(4,5)P_2$ in turn regulates three activation paths that converge on the actin cytoskeleton and secretory pathway (4–6). One path consists of a Cdc42-dependent signaling pathway (4) that regulates polarity establishment and actin organization to perpetuate exocytosis until budding is completed. A second path involves the recruitment of the GEF for Rho proteins, Rom2, by $PI(4,5)P_2$, resulting in activation of the Rho1 signaling pathway (5). Rho1 then activates Pkc1 to regulate a mitogen-activated protein kinase cascade that leads to the up-regulation of genes involved in cell wall integrity, as well as actin organization. Finally, recent studies suggest that certain exocyst components (e.g., Sec3) interact with Rho family GTPases (e.g., Rho3) and are recruited to membranes in a $PI(4,5)P_2$-dependent manner (6). This may control exocyst assembly at the site of exocytosis and facilitate secretion, among other possible functions (i.e., cortical ER delivery and anchoring). Alone, $PI(4,5)P_2$-mediated Cdc42 and Rho activation should stabilize the polarized actin cytoskeleton and, in turn, maintain both integrity of secretory pathway and facilitate further Sfh5-mediated PI delivery to the cell surface.

main altered its ability to reach the PM and to confer growth (Figure 7, B and D).

$PI(4,5)P_2$ and Cdc42 stimulate actin assembly by synergistically activating WASP proteins (Rohatgi *et al*., 1999; Higgs and Pollard, 2000), leading to Arp2/3 activation and actin nucleation/polymerization (Rohatgi *et al*., 1999). Moreover, endocytic Epsins bind $PI(4,5)P_2$ (Wendland, 2002) to regulate the level of activated Cdc42, and mutations in the epsin N-terminal homology domain result in actin defects that are rescued by the overexpression of Cdc42 effectors (Aguilar *et al*., 2006). Together with this work, it seems that *sec* pathway-mediated $PI(4,5)P_2$ synthesis modulates Cdc42 activation and thereby maintains actin organization and exocytosis until bud emergence is complete. Interestingly, the effects of Sfh5 and Mss4 upon early *sec* mutants (e.g., *sec12*, *sec22*; Figures 1, A and D, and 6, D and F) indicate that Cdc42 function is also connected to protein transport through the early secretory pathway, perhaps, via actin regulation. This idea is supported by works demonstrating that Cdc42 regulates anterograde and retrograde protein transport from the Golgi (Stamnes, 2002).

Although Cdc42 activation by the PH domain-containing GEF Cdc24 is required to orient the actin cytoskeleton toward the bud site (Toenjes *et al*., 1999), it does not mediate the exocytic signal. This is because $PI(4,5)P_2$ localization was normal in *cdc24-1* cells at elevated temperatures (Supplemental Figure S2C), unlike in *cdc42-6* cells (Figure 3A), and *MSS4* overexpression could neither ameliorate the growth of *cdc24-1* cells nor restore Cdc24-GFP localization in *sec* and *cdc42-6* mutants (Supplemental Figure S2, A and B). Thus, Cdc24 localization and function are independent of Mss4. This is supported by studies showing that the PH domain is not necessary for Cdc24 localization (Toenjes *et al*., 1999) and that Cdc42-dependent localization of polarisome components is Cdc24 independent (Rida and Surana, 2005). We determined whether the PH domain-containing Rho GEF Rom2 acts as an Mss4 effector; however, its overexpression only slightly restored the growth of *cdc42-6* or *mss4-102* cells (our unpublished data). Thus, another activator of Cdc42 confers the exocytic signal from Mss4.

What signal do the PI kinases (e.g., Stt4 and Mss4) receive to convert PI to PI(4)P and $PI(4,5)P_2$, upon vesicle fusion at the PM? One possibility is that PITPs carried by secretory vesicles present PI directly to the kinases. Routt *et al*. (2005) demonstrated a role for nonclassical PITPs (e.g., Sfh1-5) in stimulating $PI(4,5)P_2$ production through the Stt4/Mss4 pathway. Because Sfh5 delivery to the PM is dependent upon the secretory pathway and cytoskeleton (Figure 6D), and its overexpression rescues defects in secretion and Cdc42 localization (Figures 6, A and B, and 7, B and C), we propose that Sfh5 delivers PI to the PI kinases to generate $PI(4,5)P_2$. This is supported by the fact that *SFH5* overexpression improved the robustness of *mss4* cells at permissive and semirestrictive temperatures (Figure 6C) and implies that Sfh5 acts upstream of Mss4 to facilitate function but cannot replace it. Sfh5 was partly mislocalized in late *sec* mutants and severely mislocalized to endosomes (in which $PI(4,5)P_2$ accumulates upon a block in secretion; Figure 3C) in mutants of the early pathway (Figure 6, D and E). This result hints that PM-localized Sfh5 originated from early compartments (i.e., ER and Golgi). Differential centrifugation reveals that upon the temperature-shift Sfh5 accumulates in the endosome-containing P100 fraction (Figure 6, F and G), corresponding with a concomitant decrease in $PI(4,5)P_2$ and Cdc42 levels therein (Table 3 and Figures 4 and 5B). These phenomena may be connected because all of the defects are ameliorated by restored secretion or Mss4 function (Figures 4, 5B, and 6F). Finally, the mutation of residues E204 and K236 in the Sec14-like domain, which exhibits PI transfer activity (Phillips *et al*., 1999), abolished the ability of Sfh5 to enhance the growth of *mss4* cells (Figure 7B) and resulted in both Sfh5 and Cdc42 mislocalization (Figure 7, C and D). Together, the results imply that Sfh5 transits from endosomes to the PM and delivers PI to the kinases involved in $PI(4,5)P_2$ synthesis. On a block in vesicle transport, PI

delivery is reduced, resulting in decreased PI(4,5)$P_2$ production and depolymerization of the actin cytoskeleton.

Our data support a role for PI(4,5)$P_2$ in transducing a signal from the exocytic apparatus to the actin cytoskeleton via Cdc42. Interestingly, the Rho3 and Cdc42 GTPases interact directly with the exocyst (Hsu *et al*., 2004) and were suggested to confer secretory functions in an actin-independent manner (Adamo *et al*., 1999; Adamo *et al*., 2001; Roumanie *et al*., 2005). Yet, our previous work (Aronov and Gerst, 2004) and this study (Figure 2) demonstrate that their mutant alleles (e.g., *rho3-v51* or *cdc42-6*) confer significant cytoskeletal defects. In *cdc42-6*, both the cytoskeletal and growth defects were rescued by *MSS4* overexpression (Figures 1A, 2, and 5C). Although this does not preclude an actin-independent role for Rho3 or Cdc42 in secretion, it implies that Mss4 function (which controls actin) complements all defects inherent to these alleles. In addition, He *et al*. (2007) demonstrated Exo70 mislocalization in a *mss4* mutant at 37°C and proposed that PI(4,5)$P_2$ binding mediates exocyst assembly. However, we show that other factors (i.e., Cdc42 and Sfh5) also mislocalize upon Mss4 inactivation (Figure 5, A and B, and 6D); thus, it seems premature to suggest that Exo70 alone controls exocyst assembly [via PI(4,5)$P_2$ binding]. Moreover, actin delocalization alters polarized mRNA transport, which greatly contributes to the localization of soluble polarity and secretion factors (Aronov *et al*., 2007). Thus, defects in mRNA localization may also affect subunit localization. Zhang *et al*. (2008) later showed that Sec3, an exocyst subunit involved in exocytosis (Finger and Novick, 1997), ER inheritance (Wiederkehr *et al*., 2003), and mRNA anchoring to the ER (Aronov *et al*., 2007), binds to PI(4,5)$P_2$ and facilitates membrane association. Thus, two exocyst subunits (Sec3 and Exo70) were proposed to have actin-independent localization properties (Finger *et al*., 1998; Boyd *et al*., 2004) but to localize in a PI(4,5)$P_2$-dependent manner (He *et al*., 2007; Zhang *et al*., 2008). However, our work implies that PI(4,5)$P_2$ synthesis at the PM is conditional upon an intact cytoskeleton/secretory pathway. Thus, subunit localization should be sensitive to defects in actin, as has been observed (Roumanie *et al*., 2005). Moreover, because *SFH5*, *MSS4*, or *CDC42* overexpression improve the growth of temperature-shifted *sec3*Δ and *sec3-2* cells (Figures 1A, 5C, and 6A), it implies that the PI(4,5)$P_2$-driven, Cdc42-mediated, restoration of actin and secretion does not necessitate Sec3 function. Therefore, an interaction between Cdc42 and Sec3 is not essential for Cdc42 to confer exocytosis, actin regulation, and polarized growth. This would also preclude direct effects by PI(4,5)$P_2$ upon Sec3 function leading to the control of Cdc42, as has been suggested. Because Cdc42 localization to the PM is however dependent upon PI(4,5)$P_2$ synthesis (Figure 5A), we suggest that Rho GTPase and exocyst recruitment to the site of exocytosis are connected processes necessary for actin regulation (Figure 8).

## ACKNOWLEDGMENTS

We thank P. Brennwald (University of North Carolina, Chapel Hill), S. Emr (Cornell University), E. Harsay (University of Kansas), G. Jona (Weizmann Institute of Science), S. Keranen (VTT Biotechnology), P. Novick (University of California, San Diego), R. Schekman (University of California at Berkeley), and M. Wigler (Cold Spring Harbor Laboratory) for reagents. This work was supported by grants from the Minerva Foundation (Germany) and the Y. Leon Benoziyo Institute for Molecular Medicine, Weizmann Institute of Science. J.E.G. holds the Henry Kaplan Chair in Cancer Research.

## REFERENCES

Adamo, J. E., Moskow, J. J., Gladfelter, A. S., Viterbo, D., Lew, D. J., and Brennwald, P. J. (2001). Yeast Cdc42 functions at a late step in exocytosis, specifically during polarized growth of the emerging bud. J. Cell Biol. *155*, 581–592.

Adamo, J. E., Rossi, G., and Brennwald, P. (1999). The Rho GTPase Rho3 has a direct role in exocytosis that is distinct from its role in actin polarity. Mol. Biol. Cell *10*, 4121–4133.

Aguilar, R. C., *et al*. (2006). Epsin N-terminal homology domains perform an essential function regulating Cdc42 through binding Cdc42 GTPase-activating proteins. Proc. Natl. Acad. Sci. USA *103*, 4116–4121.

Aronov, S., Gelin-Licht, R., Zipor, G., Haim, L., Safran, E., and Gerst, J. E. (2007). mRNAs encoding polarity and exocytosis factors are co-transported with cortical ER to the incipient bud in yeast. Mol. Cell. Biol. *27*, 3441–3455.

Aronov, S., and Gerst, J. E. (2004). Involvement of the late secretory pathway in actin regulation and mRNA transport in yeast. J. Biol. Chem. *279*, 36962–36971.

Audhya, A., and Emr, S. D. (2002). Stt4 PI 4-kinase localizes to the plasma membrane and functions in the Pkc1-mediated MAP kinase cascade. Dev. Cell *2*, 593–605.

Audhya, A., and Emr, S. D. (2003). Regulation of PI4,5P2 synthesis by nuclear-cytoplasmic shuttling of the Mss4 lipid kinase. EMBO J. *22*, 4223–4236.

Audhya, A., Foti, M., and Emr, S. D. (2000). Distinct roles for the yeast phosphatidylinositol 4-kinases, Stt4p and Pik1p, in secretion, cell growth, and organelle membrane dynamics. Mol. Biol. Cell *11*, 2673–2689.

Boyd, C., Hughes, T., Pypaert, M., and Novick, P. (2004). Vesicles carry most exocyst subunits to exocytic sites marked by the remaining two subunits, Sec3p and Exo70p. J. Cell Biol. *167*, 889–901.

Coluccio, A., Malzone, M., and Neiman, A. M. (2004). Genetic evidence of a role for membrane lipid composition in the regulation of soluble NEM-sensitive factor receptor function in *Saccharomyces cerevisiae*. Genetics *166*, 89–97.

Desrivieres, S., Cooke, F. T., Parker, P. J., and Hall, M. N. (1998). MSS4, a phosphatidylinositol-4-phosphate 5-kinase required for organization of the actin cytoskeleton in *Saccharomyces cerevisiae*. J. Biol. Chem. *273*, 15787–15793.

Doughman, R. L., Firestone, A. J., and Anderson, R. A. (2003). Phosphatidylinositol phosphate kinases put PI4,5P(2) in its place. J. Membr. Biol. *194*, 77–89.

Downes, C. P., Gray, A., and Lucocq, J. M. (2005). Probing phosphoinositide functions in signaling and membrane trafficking. Trends Cell Biol. *15*, 259–268.

Etienne-Manneville, S. (2004). Cdc42–the centre of polarity. J. Cell Sci. *117*, 1291–1300.

Faucherre, A., Desbois, P., Nagano, F., Satre, V., Lunardi, J., Gacon, G., and Dorseuil, O. (2005). Lowe syndrome protein Ocrl1 is translocated to membrane ruffles upon Rac GTPase activation: a new perspective on Lowe syndrome pathophysiology. Hum. Mol. Genet. *14*, 1441–1448.

Finger, F. P., Hughes, T. E., and Novick, P. (1998). Sec3p is a spatial landmark for polarized secretion in budding yeast. Cell *92*, 559–571.

Finger, F. P., and Novick, P. (1997). Sec3p is involved in secretion and morphogenesis in *Saccharomyces cerevisiae*. Mol. Biol. Cell *8*, 647–662.

Gelperin, D. M., *et al*. (2005). Biochemical and genetic analysis of the yeast proteome with a movable ORF collection. Genes Dev. *19*, 2816–2826.

Goldstein, A., and Lampen, J. O. (1975). Beta-D-fructofuranoside fructohydrolase from yeast. Methods Enzymol. *42*, 504–511.

Grishanin, R. N., Kowalchyk, J. A., Klenchin, V. A., Ann, K., Earles, C. A., Chapman, E. R., Gerona, R. R., and Martin, T. F. (2004). CAPS acts at a prefusion step in dense-core vesicle exocytosis as a PIP2 binding protein. Neuron *43*, 551–562.

He, B., Xi, F., Zhang, X., Zhang, J., and Guo, W. (2007). Exo70 interacts with phospholipids and mediates the targeting of the exocyst to the plasma membrane. EMBO J. *26*, 4053–4065.

Hettema, E. H., Lewis, M. J., Black, M. W., and Pelham, H. R. (2003). Retromer and the sorting nexins Snx4/41/42 mediate distinct retrieval pathways from yeast endosomes. EMBO J. *22*, 548–557.

Higgs, H. N., and Pollard, T. D. (2000). Activation by Cdc42 and PIP(2) of Wiskott-Aldrich syndrome protein (WASp) stimulates actin nucleation by Arp2/3 complex. J. Cell Biol. *150*, 1311–1320.

Homma, K., Terui, S., Minemura, M., Qadota, H., Anraku, Y., Kanaho, Y., and Ohya, Y. (1998). Phosphatidylinositol-4-phosphate 5-kinase localized on the plasma membrane is essential for yeast cell morphogenesis. J. Biol. Chem. *273*, 15779–15786.

Hood, J. L., Logan, B. B., Sinai, A. P., Brooks, W. H., and Roszman, T. L. (2003). Association of the calpain/calpastatin network with subcellular organelles. Biochem. Biophys. Res. Commun. *310*, 1200–1212.

Hsu, S. C., TerBush, D., Abraham, M., and Guo, W. (2004). The exocyst complex in polarized exocytosis. Int. Rev. Cytol. *233*, 243–265.

Irazoqui, J. E., and Lew, D. J. (2004). Polarity establishment in yeast. J. Cell Sci. *117*, 2169–2171.

James, D. J., Khodthong, C., Kowalchyk, J. A., and Martin, T. F. (2008). Phosphatidylinositol 4,5-bisphosphate regulates SNARE-dependent membrane fusion. J. Cell Biol. *182*, 355–366.

Lechler, T., Jonsdottir, G. A., Klee, S. K., Pellman, D., and Li, R. (2001). A two-tiered mechanism by which Cdc42 controls the localization and activation of an Arp2/3-activating motor complex in yeast. J. Cell Biol. *155*, 261–270.

Lemmon, M. A., and Ferguson, K. M. (2000). Signal-dependent membrane targeting by pleckstrin homology (PH) domains. Biochem. J. *350*, 1–18.

Levin, D. E. (2005). Cell wall integrity signaling in *Saccharomyces cerevisiae*. Microbiol. Mol. Biol. Rev. *69*, 262–291.

Li, X., Routt, S. M., Xie, Z., Cui, X., Fang, M., Kearns, M. A., Bard, M., Kirsch, D. R., and Bankaitis, V. A. (2000). Identification of a novel family of nonclassic yeast phosphatidylinositol transfer proteins whose function modulates phospholipase D activity and Sec14p-independent cell growth. Mol. Biol. Cell *11*, 1989–2005.

Longtine, M. S., McKenzie, A., 3rd, Demarini, D. J., Shah, N. G., Wach, A., Brachat, A., Philippsen, P., and Pringle, J. R. (1998). Additional modules for versatile and economical PCR-based gene deletion and modification in *Saccharomyces cerevisiae*. Yeast *14*, 953–961.

Micheva, K. D., Holz, R. W., and Smith, S. J. (2001). Regulation of presynaptic phosphatidylinositol 4,5-biphosphate by neuronal activity. J. Cell Biol. *154*, 355–368.

Mousley, C. J., Tyeryar, K. R., Ryan, M. M., and Bankaitis, V. A. (2006). Sec14p-like proteins regulate phosphoinositide homoeostasis and intracellular protein and lipid trafficking in yeast. Biochem. Soc. Trans. *34*, 346–350.

Orlando, K., Zhang, J., Zhang, X., Yue, P., Chiang, T., Bi, E., and Guo, W. (2008). Regulation of Gic2 localization and function by phosphatidylinositol 4,5-bisphosphate during the establishment of cell polarity in budding yeast. J. Biol. Chem. *283*, 14205–14212.

Phillips, S. E., *et al*. (1999). Yeast Sec14p deficient in phosphatidylinositol transfer activity is functional in vivo. Mol. Cell *4*, 187–197.

Pruyne, D., Legesse-Miller, A., Gao, L., Dong, Y., and Bretscher, A. (2004). Mechanisms of polarized growth and organelle segregation in yeast. Annu. Rev. Cell Dev. Biol. *20*, 559–591.

Richman, T. J., Sawyer, M. M., and Johnson, D. I. (2002). *Saccharomyces cerevisiae* Cdc42p localizes to cellular membranes and clusters at sites of polarized growth. Eukaryot. Cell *1*, 458–468.

Rida, P. C., and Surana, U. (2005). Cdc42-dependent localization of polarisome component Spa2 to the incipient bud site is independent of the GDP/GTP exchange factor Cdc24. Eur. J. Cell Biol. *84*, 939–949.

Rohatgi, R., Ma, L., Miki, H., Lopez, M., Kirchhausen, T., Takenawa, T., and Kirschner, M. W. (1999). The interaction between N-WASP and the Arp2/3 complex links Cdc42-dependent signals to actin assembly. Cell *97*, 221–231.

Rose, M. D., Winston, F., and Hieter, P. (1990). Methods in Yeast Genetics, Cold Spring Harbor, NY: Cold Spring Harbor Laboratory Press.

Roumanie, O., Wu, H., Molk, J. N., Rossi, G., Bloom, K., and Brennwald, P. (2005). Rho GTPase regulation of exocytosis in yeast is independent of GTP hydrolysis and polarization of the exocyst complex. J. Cell Biol. *170*, 583–594.

Routt, S. M., Ryan, M. M., Tyeryar, K., Rizzieri, K. E., Mousley, C., Roumanie, O., Brennwald, P. J., and Bankaitis, V. A. (2005). Nonclassical PITPs activate PLD via the Stt4p PtdIns-4-kinase and modulate function of late stages of exocytosis in vegetative yeast. Traffic *6*, 1157–1172.

Schnabl, M., Oskolkova, O. V., Holic, R., Brezna, B., Pichler, H., Zagorsek, M., Kohlwein, S. D., Paltauf, F., Daum, G., and Griac, P. (2003). Subcellular localization of yeast Sec14 homologues and their involvement in regulation of phospholipid turnover. Eur. J. Biochem. *270*, 3133–3145.

Sha, B., Phillips, S. E., Bankaitis, V. A., and Luo, M. (1998). Crystal structure of the *Saccharomyces cerevisiae* phosphatidylinositol-transfer protein. Nature *391*, 506–510.

Stamnes, M. (2002). Regulating the actin cytoskeleton during vesicular transport. Curr. Opin. Cell Biol. *14*, 428–433.

Stefan, C. J., Audhya, A., and Emr, S. D. (2002). The yeast synaptojanin-like proteins control the cellular distribution of phosphatidylinositol (4,5)-bisphosphate. Mol. Biol. Cell *13*, 542–557.

Strahl, T., and Thorner, J. (2007). Synthesis and function of membrane phosphoinositides in budding yeast, *Saccharomyces cerevisiae*. Biochim. Biophys. Acta *1771*, 353–404.

Taverna, E., Saba, E., Linetti, A., Longhi, R., Jeromin, A., Righi, M., Clementi, F., and Rosa, P. (2007). Localization of synaptic proteins involved in neurosecretion in different membrane microdomains. J. Neurochem. *100*, 664–677.

Toenjes, K. A., Sawyer, M. M., and Johnson, D. I. (1999). The guanine-nucleotide-exchange factor Cdc24p is targeted to the nucleus and polarized growth sites. Curr. Biol. *9*, 1183–1186.

Walworth, N. C., Goud, B., Ruohola, H., and Novick, P. J. (1989). Fractionation of yeast organelles. Methods Cell Biol. *31*, 335–356.

Wendland, B. (2002). Epsins: adaptors in endocytosis? Nat. Rev. Mol. Cell Biol. *3*, 971–977.

Wiederkehr, A., Du, Y., Pypaert, M., Ferro-Novick, S., and Novick, P. (2003). Sec3p is needed for the spatial regulation of secretion and for the inheritance of the cortical endoplasmic reticulum. Mol. Biol. Cell *14*, 4770–4782.

Yin, H. L., and Janmey, P. A. (2003). Phosphoinositide regulation of the actin cytoskeleton. Annu. Rev. Physiol. *65*, 761–789.

Zhang, X., Orlando, K., He, B., Xi, F., Zhang, J., Zajac, A., and Guo, W. (2008). Membrane association and functional regulation of Sec3 by phospholipids and Cdc42. J. Cell Biol. *180*, 145–158.